The assessment of ecosystem services provided by forest edge effects on fields in a fragmented Swedish agricultural landscape

A methodological framework

Juliette Nguyen

Master Thesis 30 credits
Swedish University of Agricultural Sciences, SLU
Department of Crop Production Ecology
EnvEuro – European Master in Environmental Science
Uppsala 2022

The assessment of ecosystem services provided by forest edge effects on fields in a fragmented Swedish agricultural landscape. A methodological framework

Juliette Nguyen

Supervisor	Marcos Lana, Swedish University of Agricultural Sciences Department of Crop Production Ecology marcos.lana@slu.se
External supervisor	Henrik Meilby Copenhagen University Department of Food and Resource Economics heme@ifro.ku.dk
Examiner	Göran Bergkvist Swedish University of Agricultural Sciences Department of Crop Production Ecology Goran.Bergkvist@slu.se

Credits	30 ECTS
Level	Second cycle, A2E
Course title	Master thesis in Environmental science
Course code	EX0897
Programme	European Master in Environnemental Science
Course coordinating department	Department of Aquatic Sciences and Assessment
Place of publication	Uppsala, Sweden
Year of publication	2022
Illustration and design	Juliette Nguyen
Copyright	Juliette Nguyen
Keywords	*Carbon sequestration, cropping systems, DSSAT, ecosystem services, edge effect, food production, landscape diversification, landscape fragmentation, soil heterogeneity, soil organic carbon, spatial variability, total nitrogen, yield*.

Swedish University of Agricultural Sciences
Faculty of Natural Resources and Agricultural Sciences
Department of Crop Production Ecology

Abstract

Agricultural expansion, prompted by increasing global food demand, has fragmented, simplified, and homogenized the landscape in the last decades. The resilience and sustainability of croplands are at stake, resulting in a hight vulnerability to climate change, and having major impacts on environmental protection, biodiversity preservation and food security. As agricultural landscapes are becoming more and more homogeneous, it is essential to identify the impacts of forest edges on adjacent cropland and their provision of ecosystem services. Scientific research has shown a decrease in soil organic carbon (SOC) and total nitrogen (TN) concentration at a greater distance from hedgerows, but data and methodological studies along forest edges remain scarce.

This study was conducted to identify the spatial variability in yield across a rye field with forested edges at the Research Station of Bjertorp, Kvänum in Sweden. Ecosystem services chosen for assessment included carbon sequestration, nitrogen retention and crop production, studied through indicators such as soil organic carbon, total nitrogen, and yield, respectively.

The objectives of the study were multiple: first, to provide a methodological framework for collecting and analysing data on spatial variability in a field at the forest edge for SOC, TN and yield. Second, the ability of the Decision Support System for Agri-Technology Transfer (DSSAT) to predict this spatial variability was assessed. Finally, the identification of particular patterns in the spatial variability of each ecosystem service was discussed as well as their potential attribution to proximity to forest edges.

The methodology showed a good efficiency in the preparation of data, as the simulation was run in ArcMap and DSSAT without major inconveniences. The use of ArcMap required some knowledge of GIS but provided a useful spatial visualisation and interface for data processing. However, the predictions showed mixed results, with poor agreement between measured and predicted yield for the areas close to the field edges. A map of the yield prediction identified the need for improvements regarding the spatial variability resulting from the proximity to the forest edges. This lack of ability to depict in-field variations are assumed to be related to the lack of microclimatic data, an important factor defining the production potential. On the other hand, DSSAT forecasted a SOC accumulation in the long run with an assumed good agreement between observed and simulated data. It was difficult to capture the nitrogen cycle due to external input and crop uptake.

The collection of higher-quality data such as microclimate or site-specific soil data, as well as re-calibration, could improve the predictions accuracy. Agro-ecosystem models could also be improved to depict soil heterogeneities and tree-crop interactions.

The outcomes of this work could be used to run impact assessment studies and evaluate the effect of different landscape and land organization policies designed to increase the sustainability of food systems, resulting in new objectives of diversifying the landscape, broadening the ecosystem services to be promoted and respecting the environment

Keywords: *carbon sequestration, cropping systems, DSSAT, ecosystem services, edge effect, food production, landscape diversification, landscape fragmentation, soil heterogeneity, soil organic carbon, spatial variability, total nitrogen, yield.*

Table of contents

List of tables

List of figures

Abbreviations

AFS	Agroforestry system
C	Carbon
CAP	Common Agricultural Policy
CC	Climate change
CO2EC	Cumulative CO2 emissions from soil
CS	Cropping systems
d	Distance from the forest edge
DPNAM	Dry matter-N fertilizer productivity
DPNUM	Dry matter-N uptake productivity
DSSAT	Decision Support System for Agriculture Transfer
d-stat	Index of agreement
EF	Efficiency factor
EFS	East facing side
ESDAC	European Soil Data Center
ESSLA	Ecosystem Services in Sweden At the Landscape Level
HWAMM	Measured yield at harvest maturity
HWAMS	Simulated yield at harvest maturity
InNBal	Inorganic nitrogen balance
LNTD	Total soil litter N
N	Nitrogen
NH_3^-	Nitrate
NH^{4+}	Ammonium
NGasC	Nitrogen gas losses
NIAD	Total soil $NO_3^- + NH_4^+$
NMNC	Cumulative N mineralization
NRMSE	Normalised RMSE
N2OEC	Cumulative N2O emissions from soil
OCAM	Organic soil C at maturity
ONAM	Organic soil N at maturity
OrgNBal	Organic nitrogen balance

PD	Prediction deviation
pH	pH content
RMSE	Root mean squared error
SLU	Swedish University of Agricultural Sciences
SNBal	Soil nitrogen balance
SOC	Soil organic content
SOM	Soil organic matter
TN	Total nitrogen
WFS	West facing side
YPNAM	Yield-N fertilizer productivity
YPNUM	Yield-N uptake productivity

1. Introduction

Anthropogenically-driven climate change has slowed growth of agricultural productivity over the past 50 years in mid and low latitudes, according to the IPCC (2022). Agricultural expansion, prompted by increasing global food demand, has fragmented, simplified, and homogenized the landscape, transforming many areas of natural ecosystems into managed land (Mitchell et al., 2014; D'Acunto et al., 2016;). More and more inputs are being spread onto cropping systems to compensate for soil depletion and to address the demand for ever higher yields as well as the increasing competition for land, energy, and water (D'Acunto et al., 2016). Food production is optimized at the expense of resilience against extreme events, pests and pathogens that occur more frequently because of climate change, leading to the risk of losses and jeopardising global food security (Alberti et al., 2021; IPCC, 2022).

Agriculture is at the heart of several of this century's major challenges, namely environmental protection and biodiversity preservation, climate change and food security.

Agricultural intensification is a major cause of habitat transformation and biodiversity loss, notably through landscape fragmentation. It involves a drastic reduction in the total area of continuous intact forest, leading to restricted biome patches with zones of transition in between them (Mitchell et al., 2015). As a result, natural habitats become scarcer, most forested areas are considered to be part of transition zones, being located 90m-100m from the forest edge (Schmidt et al., 2017). This has direct consequences on the water and nitrogen cycles (D'Acunto et al., 2014; Van Vooren et al., 2018; You & Sun, 2022).

Climate change exacerbates pressures on terrestrial ecosystems supporting global food systems (Creutzig et al., 2022; IPCC, 2022). Climate change mitigation strategies aim to reduce the carbon footprint of human activities. Agriculture and associated land-use changes, responsible for about 20% of global carbon emissions (e.g. deforestation) (EPA, 2022), could play an important role in balancing anthropogenic greenhouse gas emissions through the implementation of management strategies and cropping systems that avoid carbon-releasing practices (D'Acunto et al., 2014; De Stefano & Jacobson, 2018; Viaud & Kunnemann, 2021; You & Sun, 2022).

Whilst modern agriculture has succeeded in ensuring food production in the past, it is expected to provide even more food in the coming years to meet the explosion in demand driven by population growth, but also with the shift in consumption towards meat- and dairy-based diets (You & Sun, 2022;). The lands will not be able to keep up with the frenetic pace of global demand unless alternative farming practices are implemented. The food system needs to build on more sustainable and resilient cropping systems that stop damaging the environment (Foley et al., 2005; You & Sun, 2022).

Consequently, the capacity of agricultural lands to provide ecosystem services should be emphasised. Ecosystem services are the benefits that human derive from the ecosystems (Millennium Ecosystem Assessment, 2005). Natural ecosystems usually provide the widest range of ecosystem services, while man-managed land usually targets one particular service, such as food production (Pereira et al., 2005). However, alternative multifunctional agricultural landscapes can allow for a wider range of ecosystem services delivery (Fischer et al., 2005; Rodríguez et al., 2006; Malézieux, 2012). For example, cropping systems can offer regulating and supporting services such as carbon emissions mitigation and soil and water resources protection that have important consequences on global warming mitigation (Mitchell et al., 2014; Viaud & Kunnemann, 2021; You & Sun, 2022).

Structural elements that provide shelter for wildlife and that play a role in nutrients and water cycling are essential to maintain (Mitchell et al., 2014). Indeed, cropping systems that include perennial vegetation, such as hedgerows and tree rows have already shown to improve soil quality, nitrogen and carbon nutrient supply to the field, water and nutrient retention, and thus groundwater quality (Bambrick et al., 2010; D'Acunto et al., 2014; De Stefano & Jacobson, 2018). And even though landscape fragmentation has adverse effects on several ecosystem services, isolated forest patches that remain could still benefit adjacent fields in the same way and promote landscape heterogeneity. Forest field margins could therefore play a role in providing ecosystem services that cultivated land can no longer provide.

Assessing the effects of forest edges on surrounding fields and their contribution to the natural carbon, nitrogen and water cycles would help identify whether tree-based cropping systems can be promoted for more sustainable agriculture. Research about cropping systems aim to generate scientific knowledge on ecosystem services in agriculture and integrate them into a land use perspective. Research should also aim to assess, predict, and understand carbon and nitrogen gradients from the field edge, according to Eckersten (2017).

The Decision Support Systems for Agrotechnology Transfer (DSSAT) 4.8 model used in this study is a cropping system model package that is widely recognised to simulate crop growth, development, and yield on a daily basis (Hai-

long et al., 2017; Hoogenboom et al., 2019). However, limited information is available about the use of the DSSAT model to accurately simulate the in-field variability of crop growth, as it is based on the assumption that a field is a uniform area of land (Chisanga et al., 2015; Wallor et al., 2018; Hernández-Ochoa et al., 2022;). Combined with GIS, it could be a useful tool for assessing the effects of forest edges on adjacent field at increasing distances from the edge.

1.1 Objectives

This study was carried out in the framework of the research on Ecosystem Services in Sweden at the Landscape Level (ESSLA) from the SLU´s Cropping Systems Platform, which intends to promote sustainable agricultural practices in Sweden by improving resilience and the provision of ecosystem services. The aim is to identify the type of landscape configuration to be promoted in order to improve the provision of ecosystem services and to contribute to increased sustainability of forestry and agriculture in Sweden while maintaining agricultural production (Bergkvist et al., 2015). To achieve this, knowledge of ecosystem interactions and trade-offs between ecosystem services needs to be improved.

This research intents to (1) provide a methodological framework for the assessment of ecosystem services agricultural fields surrounded by perennial vegetation, in particular food production, carbon sequestration and nitrogen retention; (2) evaluate the ability of the DSSAT process-based model to simulate within-field spatial variability of crop yields (predicted x observed yield) based on fixed initial conditions of SOC and TN concentrations for a field adjacent to a forest edge in Bjertorp, Kvänum, Sweden; (3) and discuss the potential and limitations of the model to depict the impact of forest edges on the ability of adjacent fields to provide ecosystem services, in particular food production, carbon sequestration and nitrogen retention.

1.2 Background

1.2.1 Ecosystem services

The notion of ecosystem services (ES) is a useful framework for understanding the reliance of human society on its natural environment (Foley et al., 2005). It is also central to research on agricultural ecosystems, as design and agricultural activities themselves rely on the demand for products that derive from ES (Eckersten, 2017).

According to the Millennium Ecosystem Assessment (2005), an ecosystem is "a dynamic complex of plant, animal, and microorganism communities and the non-living environment interacting as a functional unit". Ecosystems services are simply the benefits that people derive from ecosystems (Pereira et al., 2005).They have been classified according to the type of benefits they provide (Figure 1), but all directly contribute to the main constituents of human well-being, namely security, health, social relations, basic materials for a good life and freedom of choice and action (Millennium Ecosystem Assessment, 2005).

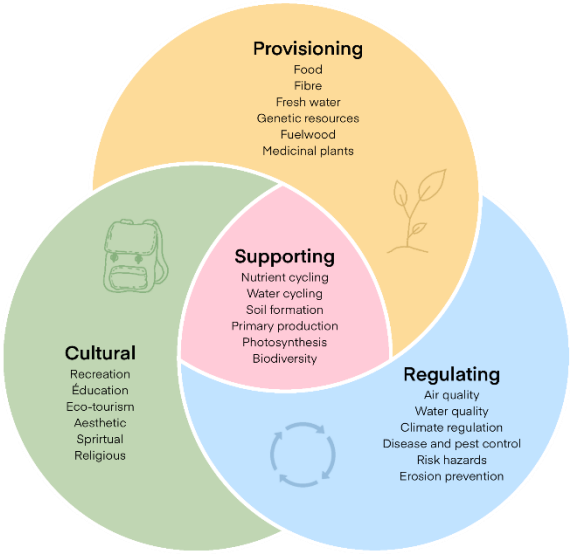

Figure 1. Classification of ecosystem services. Adapted from Kramer et al., 2022.

Since recent decades, human-induced ecological changes have been threatening the availability and reliability of ES over the long term. The climate, land cover, oceans, biodiversity and biogeochemistry of the fundamental cycles that sustain life are being modified by humans to meet the growing demand for food, fresh water, timber, fibre and fuel (Millennium Ecosystem Assessment, 2005). In addition, ecological feedbacks tend to intensify ecosystem degradation, leaving the future of ES and those who rely on them uncertain (Millennium Ecosystem Assessment, 2005; Carpenter et al., 2006).

Agriculture relies on the provision on numerous ES, in particular supportive ones such as nutrient cycles, photosynthesis, pollination, soil formation, etc (Figure 1). However, agricultural practices, focused on food supply, progressively increased pressures on ecosystems, thus compromising the ability to maintain long-term benefits (Figure 2). Overexploitation of provisioning ES has gradually degraded the regulating services that maintain air, soil or water quality, jeopardising the future yield of provisioning services (Millennium Ecosystem Assessment, 2005; Carpenter et al., 2006). In fact, most decisions about ES involve trade-offs,

where the supply of one ES is enhanced and the supply of another declines. For example, agriculture and its associated land fragmentation can improve food production but alter biodiversity, water quality and climate mitigation capacity provided by previously forested lands (D'Acunto et al., 2014; Mitchell et al., 2014). Furthermore, the use of a service such as food provision in the present, might also impact the potential of the ecosystem to deliver ES in the future, by depleting soil and water quality for future crop production (Pereira et al., 2005; Rodríguez et al., 2006; Jansson et al., 2021). Trade-offs among ES are, however, unclear, which render anticipation difficult (Carpenter et al., 2006).

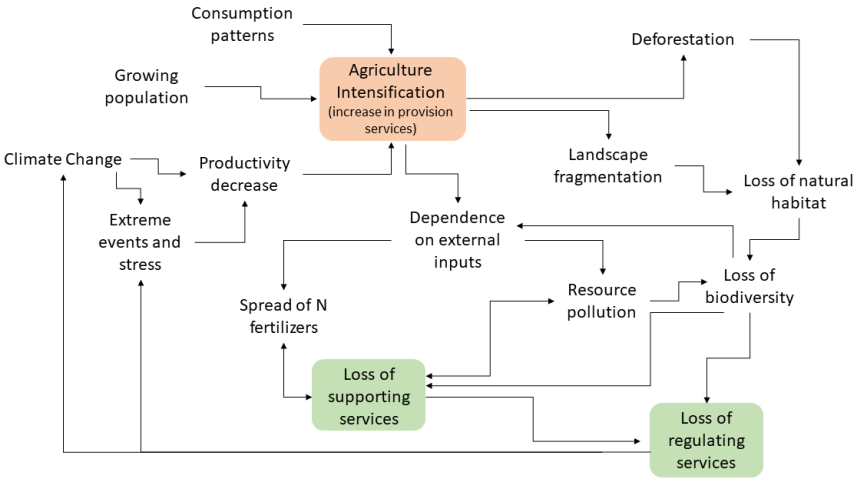

Figure 2. Drivers, consequences, and ecological feedbacks of agricultural intensification.

Overall, regulating and supporting services are neglected in favour of provisioning services because of their low visible and immediate impact (Foley et al., 2005; Pereira et al., 2005; Rodríguez et al., 2006; Mitchell et al., 2014). However, the resilience of all ecosystems relies on these types of services and their ability to moderate the impacts of extreme events and disturbances of all kinds. With the increasing intensity of human-induced shocks, ecosystems and the people who depend on them are becoming significantly more vulnerable (Carpenter et al., 2006).

Some strategies could reverse the degradation of ecosystems while meeting the increasing demand for their services. Ecological management and planning should be based on a clearer understanding of changes in ES resulting from human intervention (Carpenter et al., 2006). The management of alternative agricultural practices should promote its ability to deliver ES in the long term for use in assessing ecological sustainability (Bergkvist et al., 2015; Eckersten, 2017). However, significant changes in policies, institutions and practices would be required. The CAP 2023-2027, for example, aims to promote greener farming

practices through financial support for farmers to adopt practices that benefit the climate and the environment (European Union, 2022).

1.2.2 Carbon sequestration

Carbon (C) is one of the most common elements on Earth's biosphere. Indeed, it is an essential element for life, making up all plants and animals on the planet (Corning et al., 2016).

Soils holds the largest terrestrial reservoir of organic carbon, with an estimated total storage of more than 3~~–4~~ time that of the atmosphere (De Stefano & Jacobson, 2018; Jansson et al., 2021; Viaud & Kunnemann, 2021). Soil organic carbon is heavily correlated to soil organic matter, which is essential to soil function and productivity, generally enhancing crop yields on agricultural land. Soil organic matter also moderates erosion, nutrient leaching and improves soil aeration and water retention, thereby significantly improving soil conditions and fertility (Corning et al., 2016; Berazneva et al., 2019; Jansson et al., 2021).

Carbon sequestration, defined as "the net removal of C from the atmosphere and its deposition into a reservoir" (De Stefano & Jacobson, 2018), is part of the natural C cycle (Figure 3). In natural ecosystems, atmospheric CO_2 is taken up by plants during the photosynthesis and transformed into organic compounds that will deposit into the soil as litter and plant residues (De Stefano & Jacobson, 2018). As C is sequestered into the soil, it is less likely to escape under gaseous forms in the atmosphere (Corning et al., 2016). C transitions through various labile forms before a minor fraction enters the stabilised C pool, where it is sequestered (Jansson et al., 2021). Therefore, gaseous C emissions can originate from anaerobic decomposition (CH_4), from microbial and plant respiration (CO_2), or volatile organic compounds' (VOCs) emissions prior to sequestration. Erosion and leaching also play a role in decreasing soil organic carbon content (NASA, 2011; Corning et al., 2016; Lal et al., 2018; Jansson et al., 2021).

In agricultural ecosystems, soil amendments are usually applied through manure or fertilizer input. C is extracted from the natural cycle when crops are harvested. As agricultural soils have progressively been depleted of their original organic C pool, they are identified as having promising potential for C sequestration, through the adoption of specific management practices with adequate institutional and labour support (De Stefano & Jacobson, 2018; Jansson et al., 2021). For example, ecosystem-based approaches such as agroforestry, land restoration, agricultural diversification and precision farming can strengthen ecosystem resilience to climate change, restore ES and sustainably improve food production. They may therefore be able to preserve most of the arable land while providing many ES (De Stefano & Jacobson, 2018; Jansson et al., 2021; Viaud & Kunnemann, 2021; IPCC, 2022).

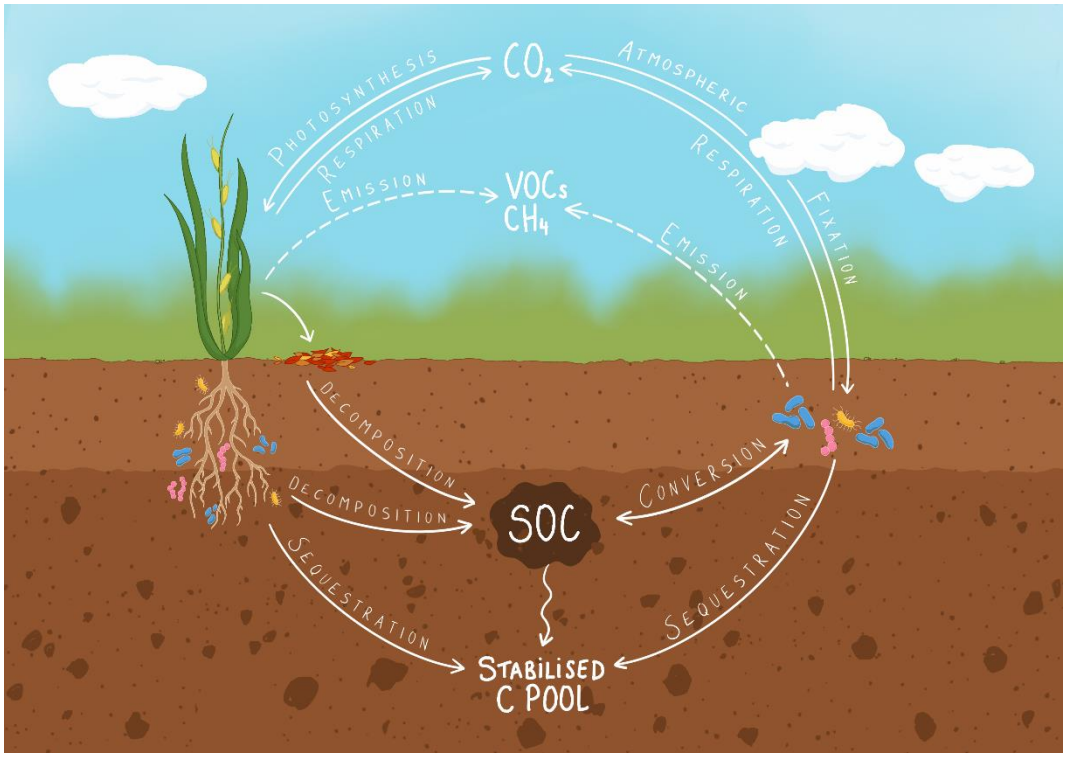

Figure 3. Carbon (C) cycle in the soil-plant-atmosphere system with a focus on soil organic carbon (SOC). Adapted from Jansson et al., 2021 and Chapin et al., 2009.

1.2.3 Nitrogen retention

Nitrogen (N) is an essential element for the development of living organisms through its assimilation into amino acids, basic bricks of proteins. It is also a constituent of nucleotides, indispensable for the formation of DNA and RNA (Knoll et al., 2012).

The most important nitrogen reservoirs are gaseous nitrogen in the atmosphere and dissolved in the ocean, and sedimentary N sealed in continental crust, which is essentially inert. However, small-scale biological fluxes, whose rates are controlled by microbes capable of fixing this mainly gaseous N, play a crucial role in the N cycle (Knoll et al., 2012).

In natural ecosystems, the rates of N supply and loss are very limited and tend to reach a steady state. The major inputs of N to the soil take place through the process of atmospheric deposition and fixation by microorganisms (Figure 4). N losses occur through leaching, erosion and surface runoff, ammonia volatilization and especially gaseous losses of N_2 and N_2O through the process of denitrification (Haynes, 1986; Johnson et al., 2005; Knoll et al., 2012).

Mineral N, which is the N available for direct plant uptake, constitutes less than 2% of the TN content of the soil. The principal forms of mineral nitrogen include ammonium (NH_4^+) and nitrate (NO_3^-), which have different mobility in soil. The

positively charged NH_4^+ ion is unlikely to leach out as it is retained in the soil by cation exchange, fixation by clay minerals and microbial immobilization. It is also nitrified relatively quickly as NO_3^-, in many cases. The NO_3^- anion, however, is readily removed from soils by leaching to groundwater or freshwater and by denitrification due to its high susceptibility to diffusion and transport in soil water (Haynes, 1986; Gikas et al., 2016).

An internal N cycle operates in the plant-soil system. Dead organic residues are microbially decomposed, resulting in the release of NH_4^+ (mineralisation), which then gets oxidised by microorganisms to NO_3^- (nitrification) for energy production. Both mineral forms of N are available for plant and microbial uptake (immobilization) (Haynes, 1986; Knoll et al., 2012). The N incorporated in their biomass then returns to the soil as detritus, which is degraded by microorganisms, fungi and invertebrates. This contributes to the formation of soil organic matter. Since most N is bound to organic compounds, its accumulation closely follows that of soil organic matter, and therefore SOC. The supply of litter, the type of vegetation and the microbial characteristics responsible for the decomposition process largely determine the N content of the soil (Haynes, 1986; Johnson et al., 2005; Knoll et al., 2012).

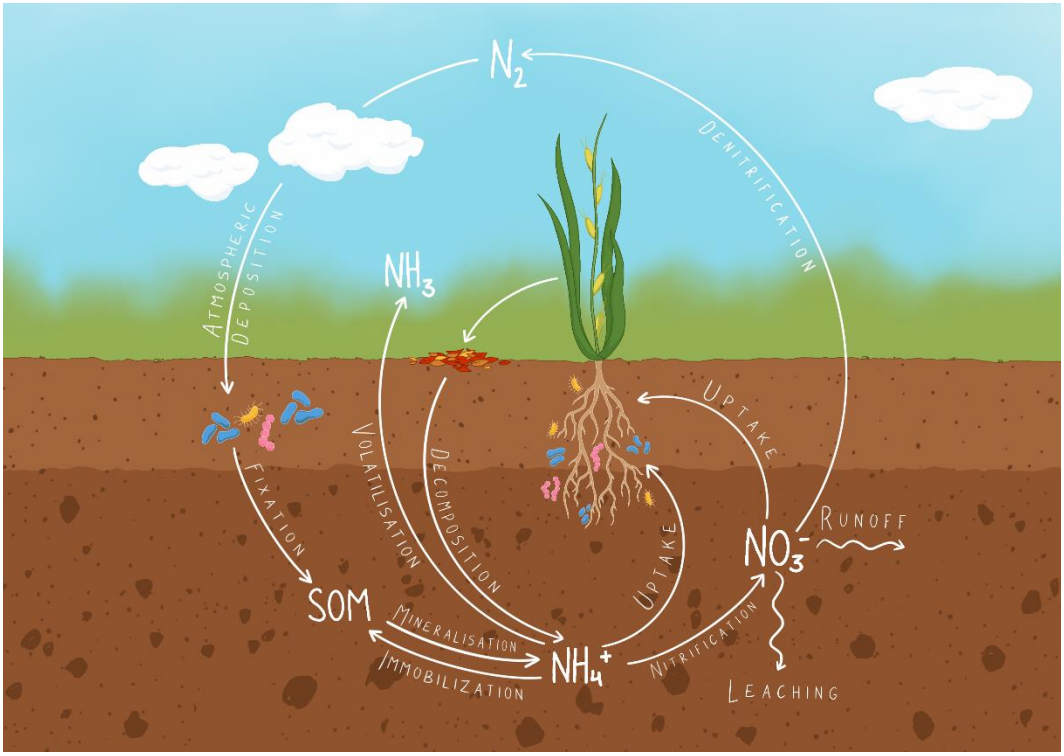

Figure 4. Nitrogen cycle in the soil-plant system. Adapted from Haynes, 1986.

In agricultural ecosystems, N availability is usually the limiting factor to crop production when soil water supply is secured. Today, agriculture is heavily reliant

on commercial synthetic nitrogenous fertilizers to sustain consistent yields despite the loss of N through plant removal. Twice as much N as is taken up by the crops is applied on crops. As a result, about half of the applied N is lost through surface and ground waters, through leaching and runoff or to the atmosphere, mainly through denitrification processes (Haynes, 1986).

Factors influencing the rate of mineralisation/immobilization are environmental parameters, but also litter quality, which is reflected in particular by the Carbon to Nitrogen (C:N) ratio, which is defined as "the ratio of the mass of carbon to the mass of nitrogen" in the soil (USDA, 2011). As soil microorganisms have a C:N ratio close to 8:1, they must acquire this proportion of each element to maintain this ratio in their organisms. However, soil microorganisms also use about 16 parts of C as an energy source, which means that they must obtain a ratio of about 24:1. If materials with a higher C:N ratio are added to the soil, a temporary nitrogen deficit will occur, and a net immobilization will result (Figure 5). Materials with a lower ratio (more N) will result in a temporary surplus of N and net mineralisation (USDA, 2011). Field edges, especially closer to perennial formations, are subjected to an external C input coming from leaves and other materials from trees, increasing the soil C content.

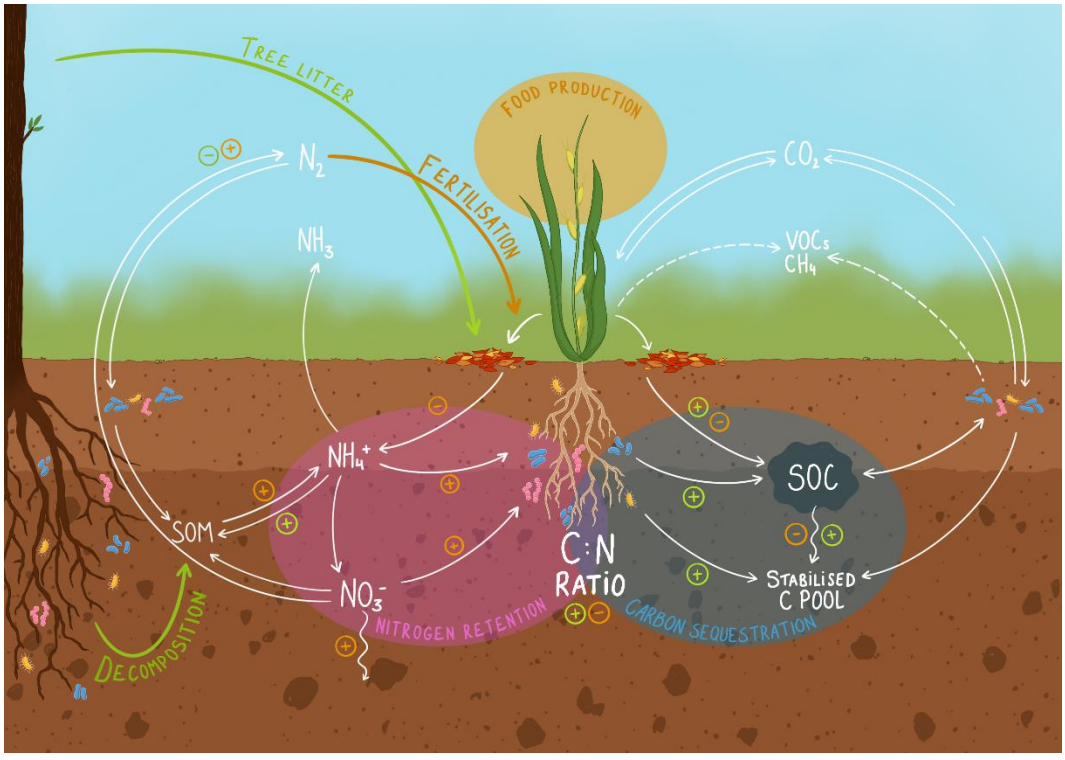

Figure 5. Coupled cycles of carbon (C) and nitrogen (N) in the soil-plant-atmosphere system and their relationship to crop growth. Potential positive (+) and negative (-) feedbacks from fertilization (Nitrogen-rich inputs) and proximity to trees (Carbon-rich inputs) on processes and carbon to nitrogen (C:N) ratio are shown in orange and green, respectively. The ecosystem services assessed are highlighted in orange, blue and purple for the food production, carbon sequestration and nitrogen retention, respectively.

1.2.4 Cropping system and landscape fragmentation

Cropping systems (CS) are defined as "the crops and crop sequences and the management techniques used on a particular field over a period of years" (Alberti et al., 2021). Although the definition may differ depending on the purpose of the research, it often includes a set of management procedures applied to a specific cultivated area (Bergkvist et al., 2015).

The productivity of an ecosystem is mainly determined by the climate (radiation and temperature) and the supply of water and nutrients from the soil (Figure 6). The potential of cropping systems to produce food depends on many factors and their interactions in the soil-plant-atmosphere system. Rabbinge (1993) has identified different levels of production related to different types of growth factors. Defining factors determine the growth potential of a crop under optimum conditions, while limiting factors are essential abiotic resources that lead to a decline in growth and yield if supplied in limited quantities. Reducing factors are biotic factors such as weeds, pollutants and diseases that inhibit growth (van Ittersum & Rabbinge, 1997).

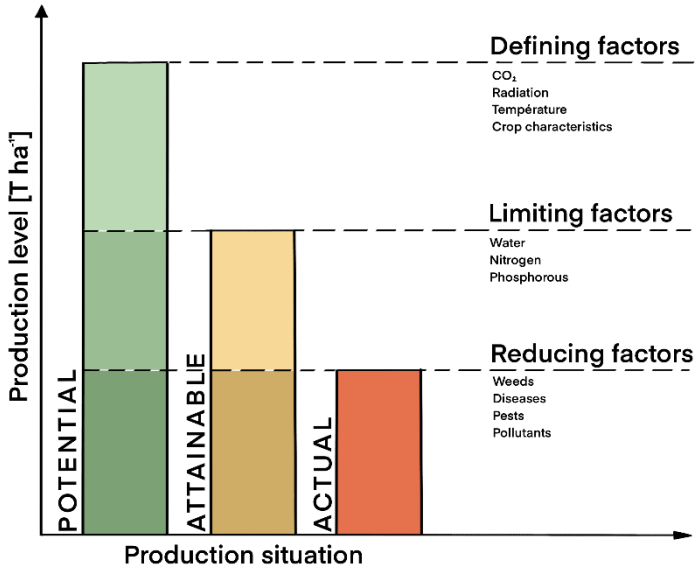

Figure 6. Factors determining crop growth. Adapted from van Ittersum & Rabbinge, 1997.

There has been an increased focus on the effects of cropping systems on soil, water and other natural resources within and adjacent to agricultural systems (Alberti et al., 2021). In this respect, ES such as water and soil quality can be used as indicators of the sustainability of cropping systems to reduce dependence on external inputs (Alberti et al., 2021). Modern cropping systems are now expected to be more sustainable, i.e., able to provide ES in the long term, and to optimise multiple functions that minimise environmental impacts on surrounding ecosystems (e.g. chemical contamination, soil loss...), while maintaining high and stable yields in a

changing climate, more independently of external inputs and non-renewable resources (Malézieux, 2012; Bergkvist et al., 2015).

Natural ecosystems can serve as a reference for the environmental and social objectives they meet while ensuring long-term sustainability. Incorporating below- and above-ground biodiversity into agricultural systems through the implementation of more complex cropping systems (crop rotation, intercropping, agroforestry) is a way to improve the delivery of ES, and overall functionality of the soil to produce crops (Figure 7) (Malézieux, 2012; Alberti et al., 2021; Hernández-Ochoa et al., 2022).

To date, the management of agricultural landscapes has generally focused on agricultural production and expansion of agricultural land, resulting in landscape fragmentation. Forest fragmentation, defined as "the breaking apart of areas of natural land cover into smaller pieces independent of a change in the amount of natural land cover" (Fahrig, 2003), results in the loss of habitats and their associated biodiversity, ES and ultimately the loss of landscape multifunctionality (Pereira et al., 2005; Mitchell et al., 2014). It is therefore necessary to encapsulate how landscape fragmentation affects the provision and flow of services according to local ecological and social components in order to develop effective tools for implementing multifunctional landscape structures. This will enable the integration of the ecosystem service concept into decision-making and planning activities (Mitchell et al., 2015).

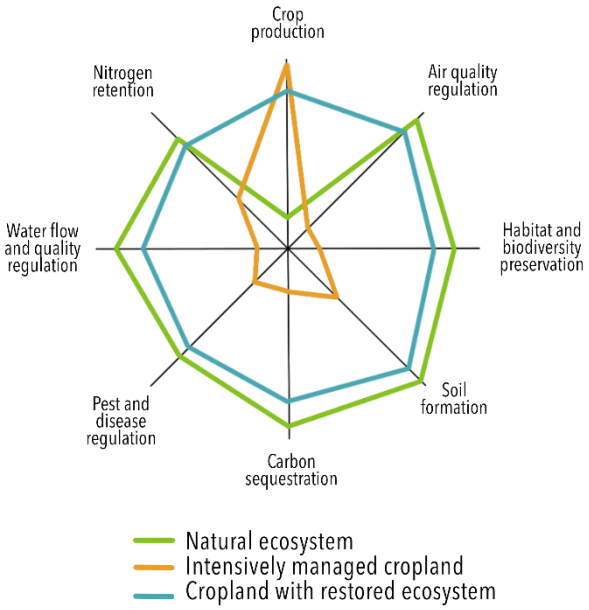

Figure 7. Web chart of hypothetical landscape impact on ecosystem services trade-offs: Natural ecosystem (green), Intensively managed cropland (orange), and Cropland with restored ecosystem services (blue). Adapted from Foley et al., 2005.

Among other farming practices, agroforestry is at the forefront of sustainable agricultural practices for climate change mitigation and ES provision (Pardon et al., 2017; Viaud & Kunnemann, 2021). Agroforestry systems are land use systems where perennial woody plants are integrated into the same land management units as crops and/or pastures under a specific spatial arrangement, in order to approximate mixed/multifunctional natural ecosystems and derive the associated benefits (ecological and economic interactions) (FAO, 2015). In agroforestry systems, the complementary use of resources by different vegetation layers and species makes it possible to provide more than one product, while avoiding or limiting compromise of the overall yield (Malézieux, 2012; Torralba et al., 2016).

Agroforestry contributes to landscape diversification and sustains production for increased social, economic, and environmental benefits while preventing most environmental damages related to agricultural expansion (FAO, 2015; Torralba et al., 2016). The presence of perennial vegetation may have a major impact in carbon sequestration, while crop dry matter only stores C for a short time, being harvested every season (De Stefano & Jacobson, 2018; Alberti et al., 2021; Drexler et al., 2021). At the same time, the addition of C residues from litter and rhizomes provides a structured, C-rich soil, improving the physical properties of the soil for crop growth and long-term ecosystem resilience, allowing microorganisms to decompose dead plant material into an increased pool of SOC (D'Acunto et al., 2014; Pardon et al., 2017; Viaud & Kunnemann, 2021).

While excess nitrogen fertiliser applied to crops leads to significant leaching of nitrogen to groundwater in conventional agriculture, this is limited in tree-based cropping systems, as the decomposition process that makes nitrogen available to plants is regulated by the continuous supply of small amounts of nitrogenous material from organic detritus.

Woody vegetation also acts as a physical barrier for water runoff and N- and P-rich sediment, limiting the erosion process that carries soil particles further into freshwaters (Torralba et al., 2016; Pardon et al., 2017). In addition, microclimatic improvements arise from the intertwined woody vegetation, playing a role in the local water cycle, notably through improved soil moisture, as well as through shading and cooling effects (Kuemmel, 2003; Mitchell et al., 2014). Agroforestry systems could become less dependent on fertilizer and irrigation inputs, making the N and water cycles more similar to those of natural ecosystems (Pardon et al., 2017).

Greater diversity in the landscape allows for greater ecosystem resilience and stability, through physical (e.g., grass strip, forest) and natural (natural enemies and (bio)diversity) barriers against pests and diseases (Alberti et al., 2021).

Agroforestry and associated landscape complexity provide biome connectivity, shelter, natural habitat, food and resources for wildlife, a necessary element for long term agricultural production and for the environment (D'Acunto et al., 2016; Torralba et al., 2016). More diverse and complex agricultural ecosystems should contribute to better belowground biodiversity and improve overall functionality for crop production (Mitchell et al., 2014; Alberti et al., 2021).

2. Materials and methods

The first objective was to provide a methodological framework on the assessment of the in-field spatial variability to provide ecosystem services. A methodological framework usually aims to "provide structured guidance on how to carry out a process or procedure using a step-by-step approach, in order to improve the consistency, robustness and reporting of the activity, improve the quality of the research, standardise approaches and maximise the reliability of the results" (McMeekin et al., 2020).

The ES selected for evaluation included carbon sequestration, nitrogen retention and food supply. The indicators considered for these ES are soil organic carbon (SOC), soil total nitrogen (TN) and yield, respectively. The values of these indicators were simulated using a processed-based crop model.

All the spatial analysis was done in ArcMap. RStudio was used for coding, and statistical analysis were performed on Excel and GBuild (DSSAT) (RStudio Team, 2022).

2.1 Data collection

2.1.1 Site description

The study focused on an agricultural field from Lantmännens farms, Bjertorp, Kvänum, in Sweden. The field was chosen due to its particularly long edge facing the forest (Figure 8) and its proximity to Bjertorp weather station (58.2644 N; 13.1132 E).

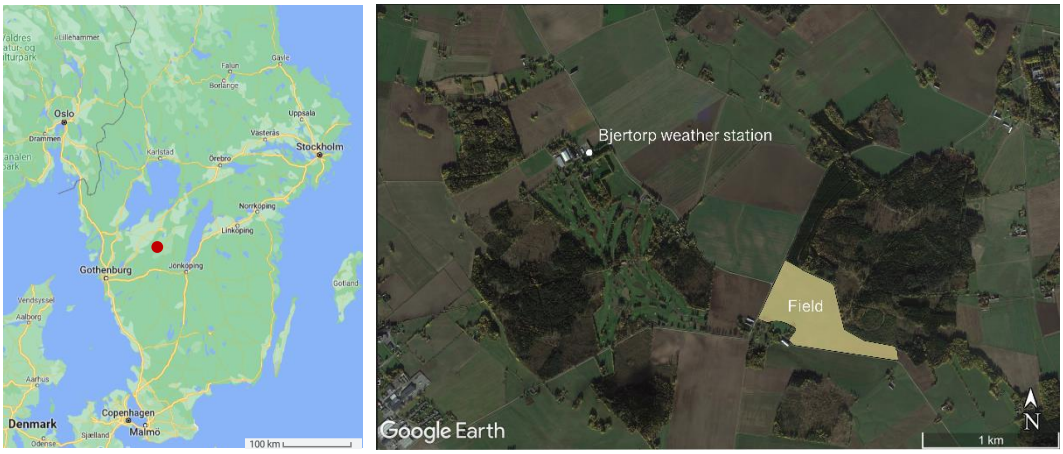

Figure 8. Map and satellite view of Bjertorp agricultural site and chosen field and weather station location.

The choice of that location offers multiple advantages for data collection. First, Bjertorp weather station has been collecting various meteorological data since 2008, which can be downloaded on LantMet (SLU, 2022); second, it is located around Lanna research station, which is an agricultural site owned and run by the SLU (SLU, 2022). Data collected through soil samples in 2010-2011, and yield data [Mg ha^{-1}], recorded by a harvester machine in 2010 were available (Soil and Environment department, SLU). The yield data had already been filtered automatically, so that the outliers were removed. Therefore, the field variations were considered accurate even though absolute values might not be.

2.1.2 DSSAT Model

The decision support System for Agrotechnology Transfer (DSSAT) crop models have been widely used to simulate crop yield of agroecological ecosystems under diverse management practices to optimize resource use and crop production while minimizing environmental damage (Soler et al., 2007; Sarkar, 2009; Chisanga et al., 2015). DSSAT is a process-based crop model that simulates the main processes occurring in the soil and plant as well as in the soil-plant system. Using a daily time step, this model is able to link weather conditions to crop growth through processes such as photosynthesis, transpiration, heat stress or frost. It simulates a one-

dimensional water balance with vertical flow to meet the requirements of relatively simple inputs for model users (Boote, 2019). It also includes database management programmes for every module that allows users to input, organise, store, retrieve and analyse crop, soil and weather data (Figure 9) (Hoogenboom et al., 2003; Alderman, 2021).

The DSSAT crop model requires the production of four separate modules with a minimum set of data for soil (1), weather (2), crop management (3) and cultivar-specific parameters (4) (Figure 9) (Jones et al., 2003; Chisanga et al., 2015; Hoogenboom et al., 2021). Since the model works for simulations on a homogeneous area of land, the field was divided into polygons comprising uniform soil properties, in order to depict the spatial variability possibly brought by the presence of forest at the border (Chisanga et al., 2015).

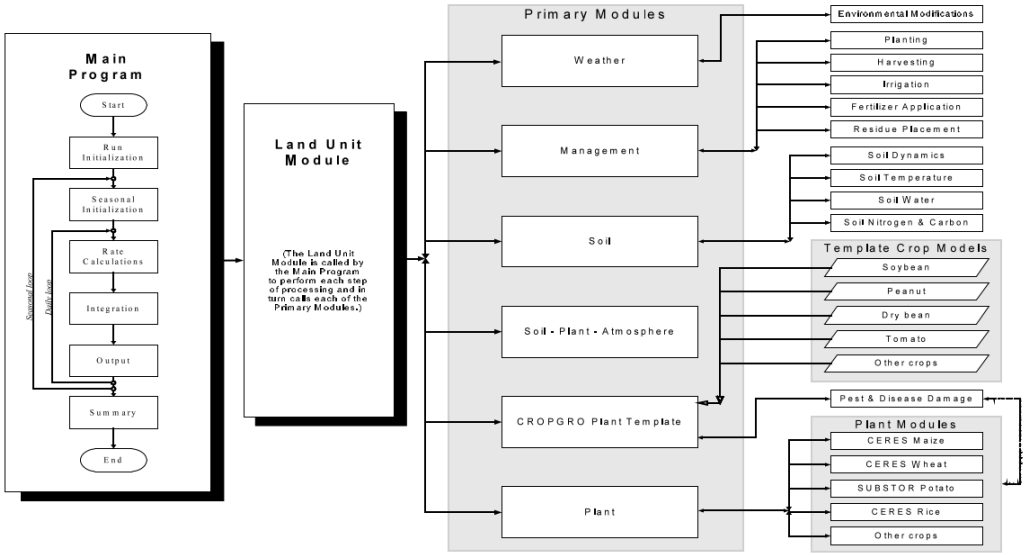

Figure 9. Overview of the components and modular structure of the DSSAT Cropping System Models (Jones et al., 2003).

2.1.3 Model input

Soil module

The minimum soil data consists of the metadata of the field location, including soil surface colour, slope, drainage and permeability, soil texture, bulk density and SOC for each soil horizon (Figure 10) (Hoogenboom et al., 2019). The TN was included in the soil parameters even though it is not part of the minimum soil data, as it is an indicator for one of the ES assessments, the nitrogen retention.

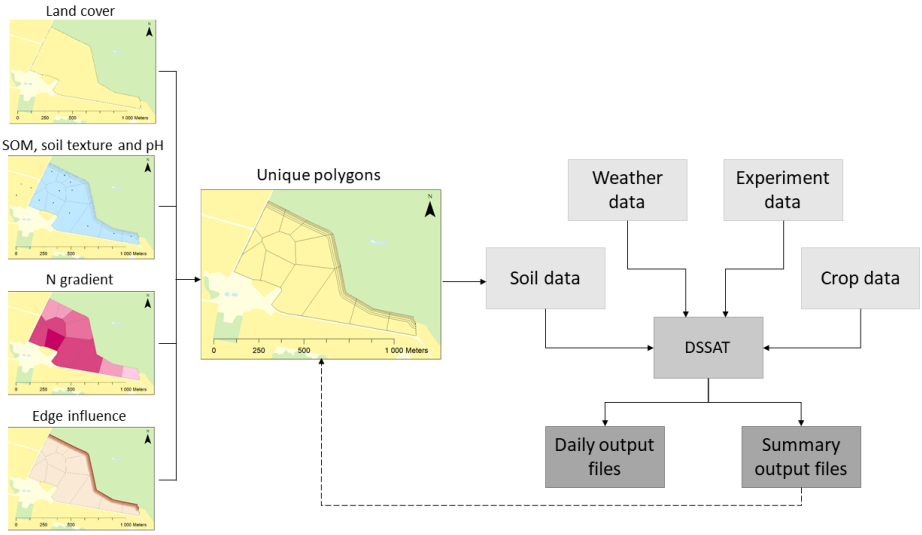

Figure 10. (Left) Soil data diagram showing the different layers of data required to highlight the forest edge effects. Land cover, forest buffer, nitrogen gradient, soil organic matter, soil texture and pH are gathered into unique polygons with a specific ID code that are imported in DSSAT. The output can be spatially compared if imported back into ArcMap.

The soil data, collected through 12 soil samples that comprised the sample location, soil texture ([%] clay and [%] silt), pH [-] and soil organic matter [%] from 2010-2011. The soil organic matter content was converted into SOC.

Soil moisture content at lower limit (LL), drained upper limit (DUL), and at saturation (SAT), and the bulk density [g/cm^3] were estimated based on textural analysis using pedotransfer functions (Kätterer et al., 2006; Chisanga et al., 2015).

The map of topsoil chemical properties based on the Land Use and Cover Area frame Survey (LUCAS) at European scale provided gridded data, with a resolution of 500m (European Soil Data Center (ESDAC), 2019; Ballabio et al., 2019) and was assumed to be the best data source available. N data was not estimated using the soil organic matter content in order to obtain independent variables.

Weather module

The minimum meteorological data encompasses the metadata of the closest weather station, such as the latitude, longitude, altitude and sensor height, as well as daily maximum and minimum temperature, precipitation and solar radiation. (Hoogenboom et al., 2019).

The weather data was downloaded on LantMet, which is a database that stores weather data from local weather stations and from the Swedish Hydrological and Meteorological institute (SMHI) (SMHI, n.d.). Bjertorp Meteorological Station, Sweden (58.2644 N; 13.1132 E), which is 1.5 km away from the field, provided minimum and maximum temperatures [°C], precipitation [mm/day] and solar radiation [W/m^2/day] since 2008.

Management module

The management module determines whether and when field operations are performed (Table 1) (Hoogenboom et al., 2003). Since the real management options were not known, those parameters were assumed based on common agricultural practices in the study region.

Table 1. Management Simulation Options.

Management options	Value	Description
Planting	R	On reported date
Irrigation	N	Not irrigated
Fertilization	R	On reported dates
Residue applications	N	No application
Harvest	M	At maturity
Tillage	N	No tillage

Cultivar module

The cultivar module includes genetic coefficients that describe "physiological processes and developmental differences among crop hybrids or varieties" (Chisanga et al., 2015). They are part of the inbuilt plant growth modules CERES-Wheat and Barley Models, that can simulate growth and yield for individual species. With the right cultivar coefficients, the CERES models can provide simulations on e.g., phenology, daily growth and partitioning, plant N and C demands, senescence of plant material, etc. (Hoogenboom et al., 2003).

Model calibration consisted in the adjustment of the genetic coefficients though "trial and error", aiming to provide simulated rye yield that compare well with observed field data (Figure 11) (Chisanga et al., 2015).

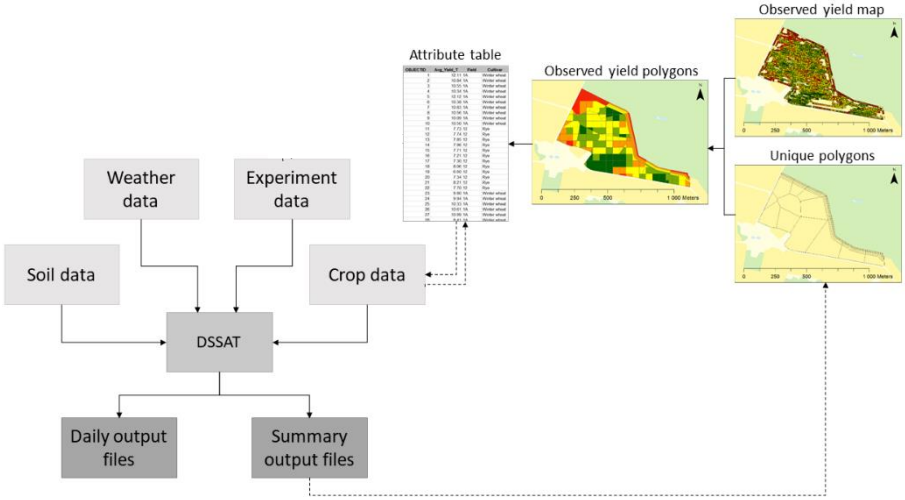

Figure 11. Crop data diagram linking the crop module and yield data. Each unique polygons holds a value for observed yield data [Mg ha^{-1}] that will be compared with the simulated yield produced by DSSAT to validate the model.

2.2 Data management

2.2.1 Data conversion and preparation

In order to better understand the topic of edge effects and ES within agricultural landscape, scientific papers were collected, using specific terms in Google Scholar and the SLU library database. Researched key words included *edge effects, field margins, transition zone, borders, boundary effect, distance-from-forest, forest edge, field-to-forest, yield response, landscape fragmentation, transect, carbon and nitrogen content, SOC, total nitrogen, gradient.*

The outcome of those papers was gathered in the background section to provide additional information on particular topics that were further developed in the discussion. However, most papers focused on the forest side of the field-to-forest boundary. The emphasis was generally on biodiversity or nutrient cycles, but no article provided a complete and site-specific assessment of the N and C concentration, comprising the local weather and soil conditions.

TN and SOC gradients

Based on the previous literature, the assumption was made that the TN and SOC content would decrease from the forest edge to the field core (Bambrick et al., 2010; D'Acunto et al., 2014; Mitchell et al., 2014; Pardon et al., 2017; Drexler et al., 2021). Data about SOC and TN concentration were needed to produce a function that could represent the gradient in concentration across the distance to the edge. Amongst the scientific papers that included useful data, studies were selected according to their location and land use type. The preferred conditions included a temperate climate as well as an arable field or meadow adjacent to any type of forest or including a woody vegetation line among the field. Furthermore, soil samples providing C or N concentrations along a transect from the edge to the core of the field were needed.

The articles found presented three different types of tree-based CS. The effects of only one of the following elements were usually identified and measured: hedges, tree lines or forest edges. Only a few studies dealt with forest edges (2 for SOC data and 1 for TN (D'Acunto et al., 2014; Schmidt et al., 2019).

Consequently, the resulting function used a combination of data extracted from studies of all three types.

For each dataset exported from the literature, it was considered that the SOC and TN concentrations were absolute (100%) at their most distant sample point from the forest edge. Each concentration was therefore divided by the concentration collected at the farthest point from the tree line, allowing for the % unit to replace the various units found in each study.

All the datasets were combined in a plot to produce a trendline function of C and N concentrations as a relation to the distance from the forest (Figure 12 Figure 13). The powered trendline provided the best fit (R^2 = 0.54 for SOC and R^2 = 0.49 for TN) and was chosen as the resulting gradient function. To implement this, it was however necessary to change the distance 0 from the field edge to 0.01 m.

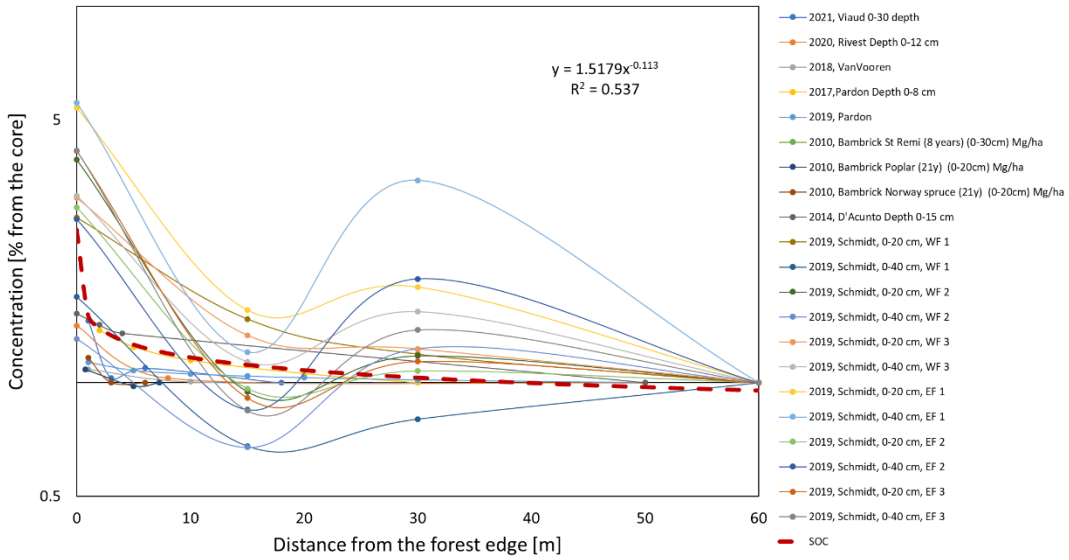

Figure 12. Combination of data on Soil Organic Carbon (SOC) concentration gradient from the edge (0m) to the core of the field (30m and onwards), with the SOC concentration in the Y axis. The data was extirped from different studies (different lines).

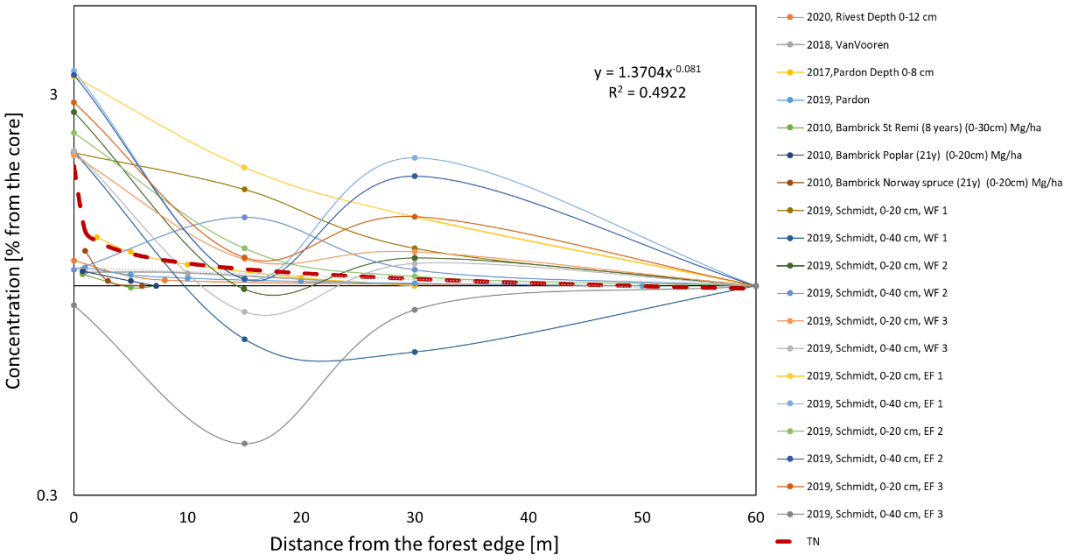

Figure 13. Combination of data on Total Nitrogen (TN) concentration gradient from the edge (0) to the core of the field (30m and onwards), with the TN concentration in the Y axis. The data was extirped from different studies (different lines).

It was chosen to highlight the spatial variability in the direct vicinity of the edge, where the concentrations tended to increase the most. Therefore, it was arbitrarily decided that the gradient function would only be considered from 2.5m up to 40m from the edge (Table 2). Beyond this distance, the SOC and TN concentrations would be considered at their minimum (100%). This prevents to getting lower values as the distance from the forest increases, and infinitely high values of SOC and TN for distances close to zero.

Table 2. Gradient function of the SOC and TN concentration (y) according to the distance from the forest edge (x), under the form $y=ax^b$..

	SOC		***TN***	
	a	***b***	***a***	***b***
From 2.5 to 40m	1.5179	-0.113	1.3704	-0.081
From 40m and onwards	1	1	1	1

Weather data

The weather data obtained from Bjertorp weather station was imported into WeatherMan, a tool provided by the DSSAT interface that allows to import, analyse and export daily weather data (Hoogenboom et al., 2019). It uses the means and variances of the imported meteorological dataset to interpolate missing and incorrect values, before creating the weather file including geographical and climatic information provided by the user (Table 3).

Table 3. Geographical and climatic parameters gathered in the weather module.

Parameter	**Value**
Latitude	58.2644
Longitude	13.1132
Climate	Humid continental climate

The quality of the single available source of microclimatic data in field edge studies (Schmidt et al., 2017) was assessed in the potentiality of deriving factors to change the local weather data in order to identify the effects of the forest edge on hydrological conditions. To do so, a statistical analysis was conducted in Excel. First, the daily weather data was calculated based on the raw hourly data. Then, the differences between the East facing side (EFS) data and the West facing side (WFS) data were calculated for each parameter (minimum and maximum temperatures, precipitation, solar radiation. Finally, these differences were analysed using ANOVA, highlighting unsignificant differences ($p>0.05$) between most parameters from the EFS and WFS. Microclimatic variations were decided not to be considered in this study, due to the lack of consistency, short series (e.g., complete growing season) recording, and the lack of significant difference between the parameters at the EFS and WFS.

2.2.2 Preparation of spatial data

Reference map and land use

The map from Lantmäteriet was used as the reference map, using SLU Geo Extraction Tool (SLU, n.d.)) to download the location around Bjertorp agricultural site. The forest and arable land attributes were extracted from the land use layer. To ensure that the forest layer never overlaps the arable land layer, the forest layer was erased from the arable land. Then, a *Multiple buffer ring* was created at regular distances from the forest, providing parallel polygons at 5, 10, 15, 25 and 35 m from the forest edge. Shorter gaps (5m) have been chosen at proximity to the edge because that is where the concentration function show the greatest slope. It was considered that the concentrations remain the same from 40m and onwards, in order to minimize the creation of unique polygons.

Soil data

The soil sample layer was added in ArcMap. Each soil sample provides measurements on the SOM [%], the soil texture [%] and the pH [-]. The SOC content [%] was deduced from the SOM value in a new field in the attribute table, according to equation 1 (WA Government, 2022). The TN was not estimated based on the SOM to prevent collinearity and provide independent variables.

$$SOM = 1.72 * SOC \quad (1)$$

The Thiessen polygon method was used to interpolate the observed data from the samples (Figure 14).

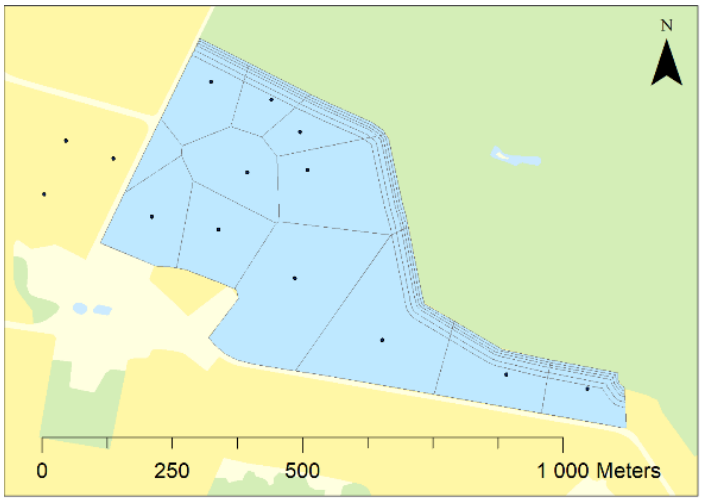

Figure 14. Unique polygons representing uniform land. Soil samples (dots) from 2010 and resulting the merge of Thiessen polygons with forest buffer rings based on distance to the forest (data from the Soil and Environment department, SLU).

As a result, for any point in the fields, parameters were equal to the observed measurements at the closest sampling location (Schumann, 1998). Sub polygons were generated, each with a constant value for each sampled parameter. The polygons newly created were merged with the forest buffer polygons in order to obtain the final configuration of polygons.

Nitrogen and vectorisation

The gridded N [g/kg soil] was imported as a raster layer (Figure 15) (Ballabio et al., 2019; ESDAC, 2019). It first needed to be vectorised, with a succession of several tools, as the *Raster to polygon* tool requires integer data only (Figure 16). Therefore, the *Raster calculator* tool first allowed to multiply the nitrogen concentration by 1000 [kg/kg]. The *Int* tool then converted each cell value of the raster to an integer (by truncation). The layer was then vectorised, using the *Raster to polygon* tool. Finally, a field (of type *float*) was added to the attribute table of each layer, using the *calculator* to fill the column with the raster values obtained above, divided by 1000. The new vector layer contained N concentrations [g/kg] with 3 decimals.

Figure 15. Gridded nitrogen concentration in percentages (500m spatial resolution) (data from ESDAC, 2019).

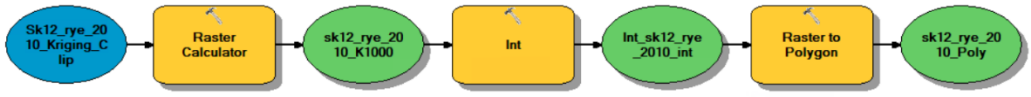

Figure 16. ArcMap model using a succession of tools to transform a raster layer into a vector layer. Blue box corresponds to model input, yellow boxes to tools and green boxes to outputs, produced in ArcMap.

N concentrations were then assimilated to each polygon by average and based in spatial location, using the *Spatial joint* tool. A new attribute field was then found in

each polygon, that corresponded to the weighted average of TN. At last, TN values were converted from g/kg into percentages [%].

Yield data

Yield data [Mg ha^{-1}] were imported into ArcMap as a text file, under the projection WGS 84. It was converted into a shapefile in ArcMap, resulting in a point feature layer (Figure 17). The yield layer was rasterised using the kriging interpolation method and clipped to the field shape.

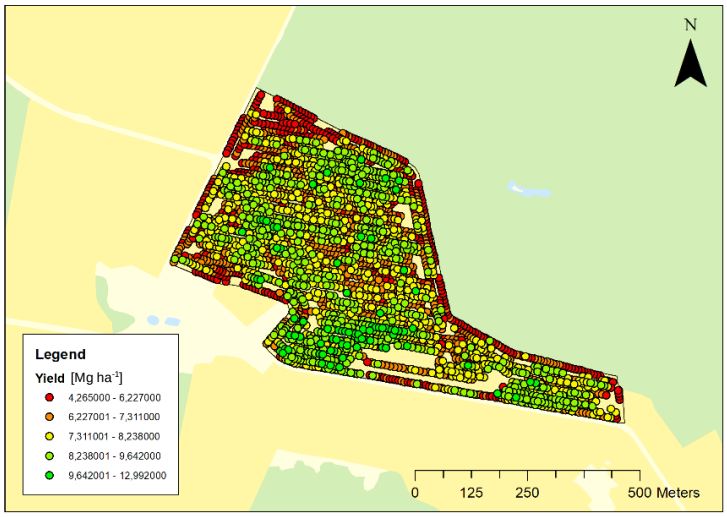

Figure 17. Yield map provided by the harvester machine and showing yield from 2010 in Mg ha^{-1} (data from the Soil and Environment Department, SLU).

Just as for the TN, the yield data was vectorised according to the steps described in Figure 16. Then, average yield data was spatially joined to each polygon through a weighted average as well. The observed yield was extracted in a table and will be compared with the yield resulting from the DSSAT simulation.

SOC and TN gradient

The mid-distances were calculated using the *field calculator (Python)* in order to find the mid-point of each buffer polygon, and to correct the default 0 distance to 40m:

```
def reclass(distance):
  if (distance == 5):
    return 2.5
  if (distance == 10):
    return 7.5
  if (distance == 15):
    return 12.5
  if (distance == 25):
    return 20
  if (distance == 35):
    return 30
  if (distance == 0):
    return 40

reclass(!distance!)
```

Henceforth, the concentration gradient was applied, depending on the mid-distance d to the forest, by adding it to the attribute table (float) according to the concentration trendlines obtained from the different papers. The resulting equations were:

If the mid-distance < 40m,

$$TN_{Grad} = TN_{Avg} * 1.3704 * d^{-0.081} \quad (2)$$

$$SOC_{Grad} = SOC_{Avg} * 1.5179 * d^{-0.113} \quad (3)$$

Otherwise,

$$TN_{Grad} = TN_{Avg} \quad (4)$$

$$SOC_{Grad} = SOC_{Avg} \quad (5)$$

This command ensured that the SOC and TN of the field were constant at the core of the field, i.e., 40m from the forest edge and beyond. All polygons were assigned a value for SOC and TN concentration, resulting in differential concentrations across the field, including higher concentrations at the forested edges (Figure 18).

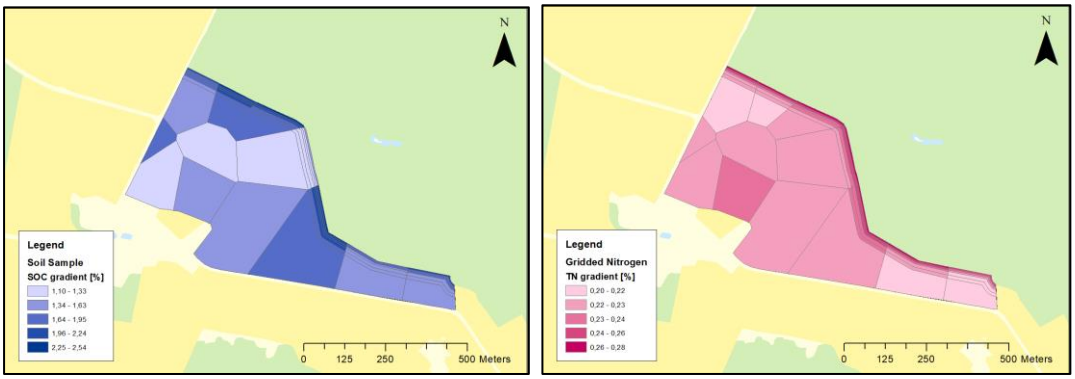

Figure 18. Cartography of the (left) Soil Organic Carbon (SOC) content and (right) Total Nitrogen (TN) concentrations for unique polygons as input for the DSSAT crop models, produced in ArcMap.

2.2.3 Finalisation of the soil file on RStudio

The soil module holds a succession of soil profiles containing the minimum soil data for every polygon, each considered as a homogeneous soil entity. DSSAT provided a typical soil profile file that can be modified in order to generate one that is specific to the assessed fields. The parameters that were collected in the previous sections therefore needed to be inserted in each polygon's soil profile. To this regard, a soil profile template file was created on the basis of the typical DSSAT file, with written code to be replaced with the specific values that were mapped in ArcMap for the topsoil layer (Table 4). The latitude and longitude are specified manually. The other parameters are estimations provided by DSSAT for Swedish soils.

Table 4. Soil module parameters.

Variable	Unit
Soil moisture content at saturation (SAT)	cm^3/cm^3
Soil moisture content at lower limit (LL)	cm^3/cm^3
Soil moisture content at drained upper limit (DUL)	cm^3/cm^3
Bulk density	g/cm^3
SOC	%
Clay	%
Silt	%
TN	%
pH	-

Pedotransfer functions provided a useful estimation for drainage and permeability characteristics on the basis of soil texture and SOC. Estimates were added in the attribute table in Excel according to the following equations (Kätterer et al., 2006):

Soil moisture content at saturation (SAT)(cm^3/cm^3):

$$SAT = -0.33 * sand + 0.46 \quad (6)$$

Soil moisture content at lower limit (LL) (cm^3/cm^3):

$$LL = 0.44 * clay + 0.025 \quad (7)$$

Soil moisture content at drained upper limit (DUL)(cm^3/cm^3):

$$DUL = 0.30 * silt + 0.12 \quad (8)$$

Bulk density (g/cm^3):

$$\rho = -0.19 * SOC + 1.82 \quad (9)$$

The attribute table was saved as a csv file with the unique polygons' codes as head row. The number format (Ex: 1.234 has five characters) needed to coincide with the number of characters from the code (Ex: _SLLL has five characters).

To automate the process, a code (Appendix 1) was produced in RStudio. It enabled to successively replace the parameters' values in the soil profile template with the ones of each polygon from ArcMap. The soil file was progressively being created by appending the soil profiles one after the other.

The soil file obtained contained 47 soil profiles that corresponded to the 47 unique polygons constituting the field in Bjertorp. The first soil profiles can be found in the Appendix (2).

2.2.4 Crop modelling calibration

Once the soil and weather data files preparation were completed, the field conditions were replicated in CSM-CERES model to start the calibration process.

Observed yield data (from Figure 17) was used as a base for the estimation of DSSAT generic genotypes that is part of the calibration process. In order to estimate the rye genetic parameters, a Bayesian method was employed (Boote, 1999). This method uses Monte Carlo sampling from prior distributions of the coefficients and a Gaussian likelihood function to choose the ones that best match the observed values. The advantage of this approach is to combine information of different observations to estimate the distribution probability of parameters values and model predictions (Beven & Freer, 2001). To achieve this task, the Generalized Likelihood Uncertainty Estimation (GLUE) methodology was employed (He et al., 2010). The process was initially run only for developmental parameters (assuming the 15th of April as sowing date and the harvest date minus two weeks as the physiological maturity date) to correctly simulate the plant phenology (based on the thermal sum of different stages).

Once the model was able to mimic the observed physiological maturity date with less than 10% error, growth coefficients (maximum number of kernels per plant and grain filling rate), were calculated. The overall procedure was done using 30000 runs of the model and using 2/3 (31) of the polygons for calibration and 1/3 for an independent validation. Polygons for model calibration and validation were randomly selected. Each simulation run generated indexes to compare the simulated and observed values in all the individual polygons.

At the end of the process, the set of genetic coefficients with higher probability of matching the observed values was selected by GLUE and used to generate the yields (Appendix 3).

2.3 Data analysis

2.3.1 Evaluation of the methodological framework

Once the model generated yields for all polygons, the attribute table of the shape file was edited on OpenOffice to include new columns related to yield. The observed [%] and predicted [kg ha^{-1}] SOC were mapped in the same way.

As for the TN concentrations, a correlation table was produced with possible variables for comparison. The variables with highest correlation were plotted and mapped in ArcMap. They included cumulative N mineralization and cumulative N immobilization [kg ha^{-1}].

The meteorological data (Figure 19) shows a typical Swedish weather with cold and dry days in winter, humid spring, and warm temperatures in summer. Important rain events occurred in the summer, indicating that in this year crops probably did not suffer any intense stress related to drought or higher temperatures.

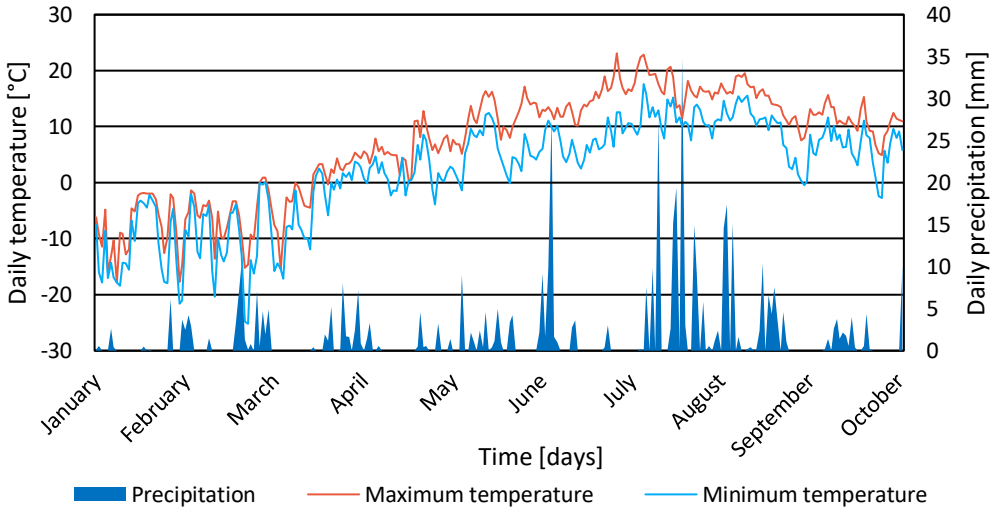

Figure 19. Weather conditions for year 2010 at Bjertorp weather station, Kvänum, Sweden.

2.3.2 Evaluation of DSSAT models performance

For model evaluation, the simulated rye yield was compared with the observed values of 2010. Since the model outputs (predicted yield) are produced with 0% moisture, the observed yield data was adjusted to reflect this (HWAMM variable). The measured yield is based on a yield map shown in the previous section (Figure 17).

Even though statistical tests (e.g., regression) are a common tool for model evaluation, distance measures were considered more appropriate in this study. Wallach et al. (2019) found that system models do not necessarily satisfy the assumptions (e.g., normality) on which those tests are based. In addition, the amount and variability of data affects the acceptance of the model. But most importantly, mathematical models are tools for simplifying the complex reality of agronomic processes. Even with sufficient data, models remain estimates and the null hypothesis would be rejected in all cases. Quantitative measures of how well the model simulates the data therefore seem more appropriate than tests at arbitrary levels (Wallach et al., 2019).

Therefore, performance statistics were determined to assess the model predictions quality. They included the root mean square error (*RMSE*) and

normalised *RMSE* (*NRMSE*), the index of agreement (*d-stat*) and model efficiency (*EF*) as recommended by Wallach, Makowski, Jones, & Brun (2019).

$$RMSE = \sqrt{\frac{1}{n}\sum_{1}^{n}(P_i - O_i)^2} \tag{10}$$

$$NRMSE = \frac{RMSE}{M} \times 100\% \tag{11}$$

$$d - stat = 1 - \frac{\sum_{i=1}^{n}(P_i - O_i)^2}{\sum_{i=1}^{n}(|P_i'| - |O_i'|)^2} \tag{12}$$

$$EF = 1 - \frac{\sum_{i=1}^{n}(P_i - O_i)^2}{\sum_{i=1}^{n}(P_i - M)^2} \tag{13}$$

With n as the number of observations, P_i and O_i referring to the predicted and observed values and M to the mean of the observed variable. P_i' and O_i' corresponded to $P_i - M$ and $O_i - M$, respectively.

The *RMSE* allows to determine statistical differences between predicted and measured values. The *NRMSE* gives a relative measure of the residual variance of the model, with a prediction considered excellent [%] if the *NRMSE* < 10%; good if 10% < *NRMSE* < 20%; fair if 20% < *NRMSE* < 30%; and poor if *NRMSE* > 30%, according to (Hoogenboom et al., 2003). The closest index of agreement *d-stat* to one, the better the agreement between the measured and simulated variables. The EF determines the goodness of fit with the best degree of fit at 1. A value of 0 would indicate an equal fit to P_i=M and negative values an even worse fit (Mayer & Butler, 1993; Wallach et al., 2019).

The prediction deviation (PD) [%] was calculated for each prediction, using the following equation:

$$PD = \frac{O_i - P_i}{O_i} \tag{14}$$

Where *Oi* and *Pi* are the observed and predicted values, respectively. Therefore, the *PD* indicates an underestimation if it is negative and vice versa (Soler et al., 2007).

2.3.3 Effects on selected ecosystem services

The output files regarding SOC and TN included data with different concentrations than those of the input files, and normalization (V_{norm}) was required to allow plotting and comparison (Developers, Google, 2022).

$$V_{norm} = \frac{(V_i - V_{min})}{(V_{max} - V_{min})} \quad (15)$$

Where V_{min} and V_{max} are the minimum and maximum of the values considered.

The predicted normalized error (PNE) was calculated to highlight the difference between normalized observations and simulations.

$$PNE = NOSOC - NPSOC \quad (16)$$

With *NOSOC* and *NPSOC* being the normalzed observed and predicted SOC, respectively.

3. Results

3.1 Methodological framework

In the existing literature on effects of perennial vegetation on agricultural fields, hedgerows were the most studied structural element, compared to forest edges and tree rows. However, similar effects were described regarding their impacts on SOC and TN concentrations on adjacent lands. The data found on the three types of structural elements were combined to generate concentration curves for SOC and TN at increasing distances from forest edges (Figure 20). Both resulting functions show a similar decrease, with a slightly more abrupt slope for TN. Both curves reach 100% around 40m from the forest edge (100% SOC= 40m and 100% TN= 50m). This leads to a percentage error of 0.05% for SOC and 1.64% for TN.

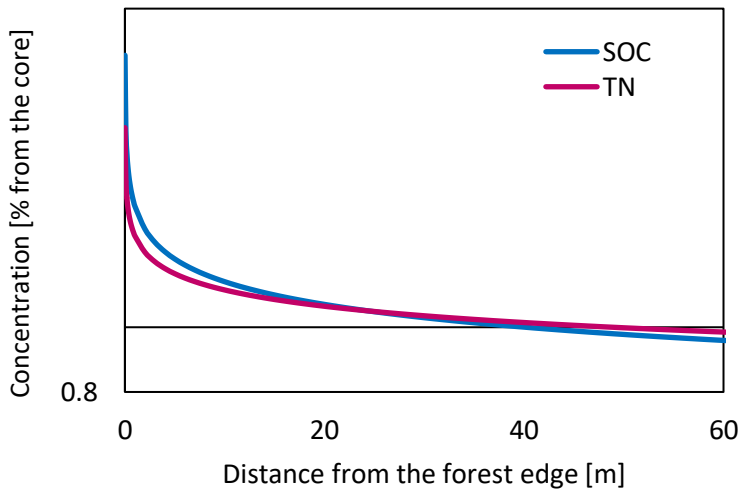

Figure 20. Concentrations curves of Soil Organic Carbon (SOC) and Total Nitrogen (TN) in relation with the distance to the forest. Based on literature data on hedgerows, tree rows and forest edges and their effects on carbon and nitrogen concentrations on adjacent land.

The correlation table (Table 5) indicates a strong correlation with the distance from the forest edge *d* with the TN, with a smaller effect on SOC, suggesting that the gradient function was able to match the TN and SOC "observed" values. Yield, however, shows quite a highly positive correlation with distance from the forest

edge (r=0.69), illustrating very clearly the spatial heterogeneity in the field. TN and SOC have a negative correlation with yield, supporting the fact that a decrease in TN and SOC is observed when yields increase and inversely.

Table 5. Correlation table between input variables and ecosystem services indicators. The colour gradient show where the value of each cell falls within the selected range, with red and green highlighting the strongest correlations (negative and positive).

	pH	*clay*	*sand*	*silt*	*d*	*LL*	*DUL*	*SAT*	*BD*	*TN*	*SOC*	*Yield*
pH	1.00											
clay	0.96	1.00										
sand	-0.97	-0.95	1.00									
silt	0.92	0.87	-0.98	1.00								
d	-0.06	-0.08	0.09	-0.09	1.00							
LL	0.96	1.00	-0.95	0.87	-0.08	1.00						
DUL	0.92	0.87	-0.98	1.00	-0.09	0.87	1.00					
SAT	0.97	0.95	-1.00	0.98	-0.09	0.95	0.98	1.00				
BD	0.29	0.27	-0.19	0.13	0.57	0.27	0.13	0.19	1.00			
TN	-0.11	-0.08	0.09	-0.09	-0.86	-0.08	-0.09	-0.09	-0.54	1.00		
SOC	-0.29	-0.27	0.19	-0.13	-0.56	-0.27	-0.13	-0.19	-1.00	0.54	1.00	
Yield	0.28	0.26	-0.32	0.34	0.69	0.26	0.34	0.32	0.50	-0.56	-0.49	1.00

d: distance from the forest edge, LL: Soil moisture content at lower limit, DUL: Soil moisture content at drained upper limit, SAT: Soil moisture content at saturation, BD: Bulk density, TN: Total nitrogen, SOC: Soil organic content.

Soil pH and texture (reflected by clay, silt and sand) are found to have a non-negligible correlation with yield (negative for sand), as well as with SOC. However, no significant correlation was found between soil characteristics and TN. Soil moisture contents (LL, DUL, SAT) also show a positive correlation to yield.

From this table, it is evident that pH and soil texture are strongly correlated, suggesting a high degree of collinearity, which should be taken into account for an appropriate interpretation. Indeed, the percentages of silt, sand and clay are linked together by the soil texture diagram, summing up to 100% for each soil profile.

3.2 DSSAT models performance

The appendix (3) shows the genotype coefficients generated by the GLUE (DSSAT model) after calibration.

The Figure 21 (left) reveals that the model tends to overestimate the yield. In addition, the scatter of the points shows a curved pattern that deviates from the 1:1 trend line. The presence of horizontal lines indicates that some of the polygons had

the same soil and weather data, which lead the model to produce the exact same yields.

And whilst the observed yield had a mean of 5875 kg ha^{-1} and a standard deviation of 639 kg ha^{-1}, the predicted dataset showed a greater mean (6241 kg ha^{-1}) and a lower standard deviation (354 kg ha^{-1}). This is reflected by the Figure 21 (right), which highlights a greater variability in the observed dataset, that was not accurately depicted by the model.

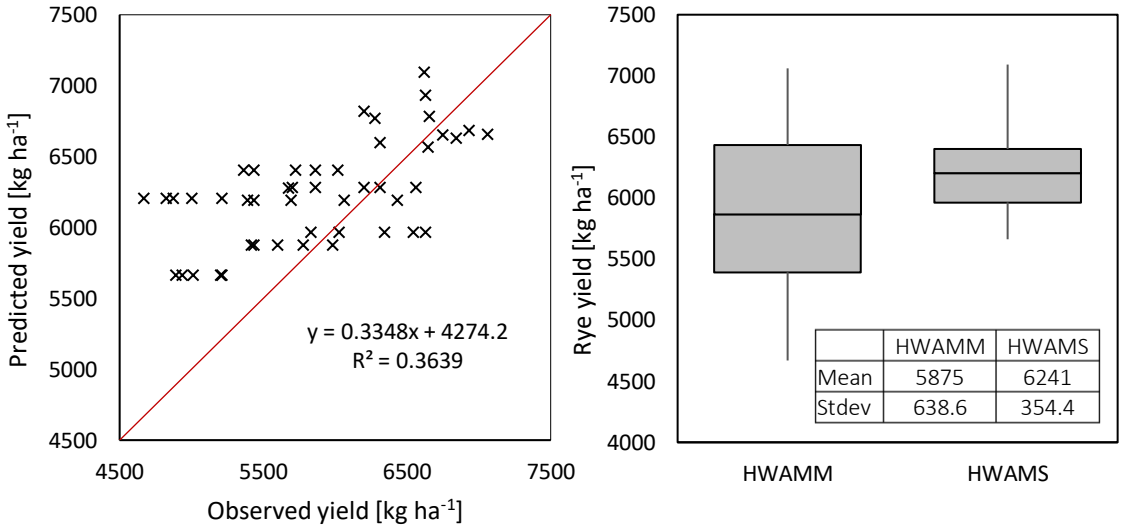

Figure 21. (Left) comparison of measured and predicted rye yield (2010). (Right) box plot comparing minimum, 1st quartile, median, 3d quartile and maximum values for measured (HWAMM) and simulated (HWAMS) rye yield at maturity.

The R^2 suggests that the model was not able to depict much variation from the observed variable) (Table 6). However, the prediction is considered close to excellent with a NRMSE of 10.7 % (Hoogenboom et al., 2003). The index of agreement *d-stat* (0.662) suggests that the model provides a good fit for the observed yield. According to Mayer & Butler (1993), the negative *EF* (-0.52) reflects a worse fit to the data than $P_i = M$.

Table 6. Model performance statistics based on the comparison of observed and predicted rye yield for 2010.

Model performance statistics	**Value**
R^2	0.364
RMSE	627.87
NRMSE [%]	10.7
d-stat	0.662
EF	-0.519

R^2, coefficient of determination; *EF*, forecasting efficiency; *d-stat*, index of agreement; *RMSE*, root mean square error; *NRMSE*, normalized *RMSE*

The prediction deviation ranged from -33% to 11%, which indicates that the model tended to overestimate the yields (Figure 22, left). Most predictions, however, fall in between 10 and -10%, suggesting a fair fit for most observations. Most field core polygons have accurate predictions (<|5%| and <|10%|) and that the poorest predictions are mostly found at the forest edge, with important overestimations (*PD* < 0).

The observed yields at the field core (dark green areas) seem to be relatively high, which was well depicted by the simulation (Figure 22, right). However, the polygons at the edges show a lower yield that is less accurately predicted. No low values at all were predicted by the model, illustrating the model's tendency to overestimate the yields, especially at shorter distances to the forest edges. The upper left corner shows particularly low yields.

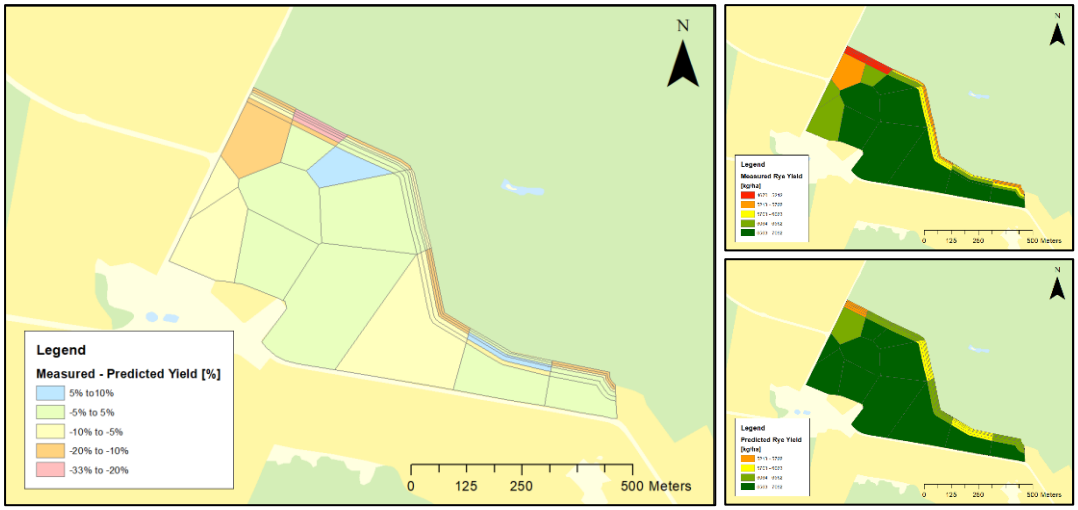

Figure 22. (Left) prediction deviation (PD) calculated via equation 10. Green colour indicates an absolute predicted deviation of less than 5%. Blue colour indicates an underprediction of more than 5% and yellow to red colours indicate an overprediction of 5% to 33%. (Right) Cartography of the measured yield (above) and simulated rye yield (below) for 2010, at studied site, Bjertorp, Kvänum, Sweden. Yellow to red colours show relatively low yields while light and dark green show relatively high yields.

3.3 Ecosystem services

3.3.1 Food production

Food production provision was assessed in the previous section through the model evaluation that compared the observed and predicted yield at maturity [kg ha^{-1}]. The results show a poor agreement between the observed and predicted datasets, suggesting that the model should be recalibrated to try and provide a better fit.

The simulated yield (*HWAMS*) shows some good correlation with a few variables (Table 7). The pH and soil texture demonstrate a significant correlation

with the measured yield (positive and negative). In addition, the distance from the forest has a great correlation with both the measured and simulated yield, indicating that the model was able to depict some of the effects of the forest edge on food production. Both yield variables show a similar negative correlation with observed TN. The N leached during season (*NLCM*) also shows a nearly equal correlation to *HWAMM* and *HWAMS* (0.34 and 0.32), respectively. *CO2EC*, which corresponds to the cumulative CO_2 emissions from soil, is highly correlated to *HWAMS*, and fairly correlated to *HWAMM*.

Furthermore, the NGasC and organic nitrogen (*ONAM*) have a close to zero correlation with both yield datasets.

Most of the variables seem to behave differently with regard to observed or simulated yield.

Several variables show a relatively high negative correlation to *HWAMM*, while showing a significantly lower correlation to *HWAMS* (OrgNBal, *NIAD*, *NMNC* and *NIMC*). On the contrary, the variables that are positively correlated to *HWAMS*, are not as much correlated to *HWAMM* (*InNBal*, *SNBal*, *N2OEC*).

Table 7. Correlation table with initial harvest yield at maturity (HWAMM) and simulated harvest yield at maturity (HWAMS) against various input and output variables. The colour gradient show where the value of each cell falls within the selected range, with red and green highlighting the strongest correlations (negative and positive).

	HWAMM	HWAMS
pH	0.28	0.09
clay	0.26	0.04
sand	-0.32	-0.15
silt	0.35	0.20
d	0.69	0.61
TN	-0.56	-0.42
SOC	-0.49	-0.03
OCAM	-0.54	-0.16
InNBal	0.08	0.40
OrgNBal	-0.44	-0.25
SNBAL	-0.01	0.30
NIAD	-0.32	-0.22
NLCM	0.34	0.32
NGasC	0.04	-0.04
NMNC	-0.61	-0.21
NIMC	-0.61	-0.03
LNTD	0.12	0.30
ONAM	0.00	0.04
N2OEC	0.08	0.26
CO2EC	0.48	0.87

d: distance from the forest edge, TN: Observed Total Nitrogen, SOC: Observed Soil Organic Carbon, OCAM: Predicted Soil Organic Carbon, InNBal: Inorganic Nitrogen Balance, OrgNBal: Organic Nitrogen Balance, SNBAL: Seasonal Nitrogen Balance, NIAD: Total soil NO_{3^-} + NH_4^+, NLCM: N leached during season, NGasC: N Gas losses, NMNC: Cumulative N mineralization, NIMC: Cumulative N immobilization, LNTD: Total soil litter N, ONAM: Organic N at maturity, N2OEC and CO2EC: Cumulative N_2O and CO_2 emissions from soil

3.3.2 Carbon sequestration

There is a good fit between the observed and predicted values (R^2 = 0.97). However, the scatter plot (Figure 23) proves the tendency of the model to overestimate the SOC at maturity, as most points lie above the 1:1 trend line.

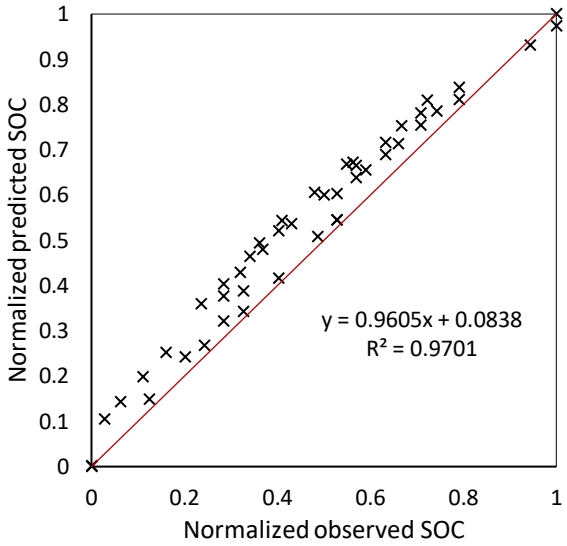

Figure 23. Comparison of normalized measured and simulated soil organic carbon (SOC) for 2010 at the studied site, Bjertorp, Kvänum, Sweden.

The Figure 24 (left) displays the spatial variability across the field. Although the variables have different units, the two maps show a very similar pattern, with relatively higher values near forest edges. The model seems to have predicted the SOC with accuracy. However, the Figure 24 (right) highlights the almost systematic over-prediction of the model. Only a few points are located above the zero line. In general, the predicted normalized error (PNE) vary from 0.03 to -0.14. Greater gaps are found close to forest edges.

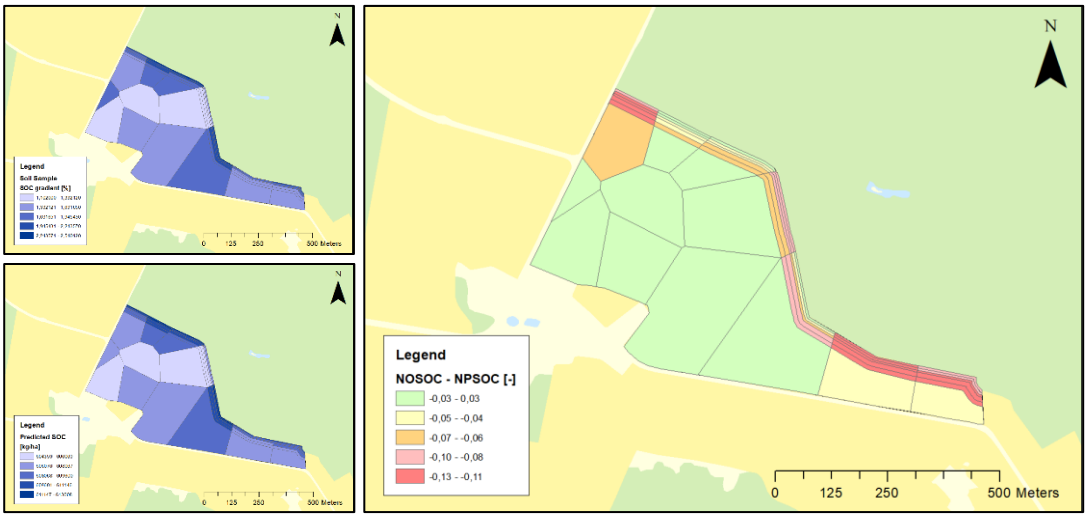

Figure 24. (Left) cartography of the initially observed SOC gradient in % (above) and the predicted SOC at the end of the season in kg ha^{-1} (below), in 2010, at the studied site, Bjertorp, Kvänum, Sweden. Light to dark blue colours indicate relatively low to high concentrations, respectively. (Right) difference between normalized observed SOC (NOSOC) and normalized predicted SOC (NPSOC) calculated according to equation 16 (method section).

The correlation between *OCAM* and SOC is extremely strong (Table 8). For both the *OCAM* and *CO2EC*, the model was able to depict the relation with forest edge, as indicated by the relatively high absolute coefficient of correlations (r=-0.63 and r=0.62, respectively). No significant correlation was found for *OCAM* and *CO2EC* with pH and soil texture. *CO2EC* appears to show an important correlation to both observed and simulated yield (*HWAMM* and *HWAMS*).

Table 8. Correlation table comparing organic carbon at maturity (ONAM) and cumulative CO_2 emissions from soil (CO2EC). The colour gradient show where the value of each cell falls within the selected range, with red and green highlighting the strongest correlations (negative and positive).

	OCAM	CO2EC
TN	0.55	-0.35
SOC	0.98	-0.06
HWAMM	-0.54	0.48
HWAMS	-0.16	0.87
pH	-0.29	0.00
clay	-0.28	0.03
sand	0.19	0.01
silt	-0.12	-0.03
d	-0.63	0.62

TN: total nitrogen, SOC: Soil organic carbon, d: distance from the forest edge, HWAMM: initial harvest yield at maturity, HWAMS: simulated harvest yield at maturity

3.3.3 Nitrogen retention

As, the model did not provide an output equivalent to TN, several variables could be candidates for comparison.

Most of the N variables are positively correlated with TN (Table 9). However, only a few shows a significant correlation with TN (positive or negative. They include the cumulative N mineralization (*NMNC*) [kg ha^{-1}], cumulative N immobilization (*NIMC*) [kg ha^{-1}] and Organic N at maturity (*ONAM*) [kg ha^{-1}]. The SOC exhibits greater correlations with N-related model output variables. Most N variables are correlated with pH and soil texture (clay, sand and silt).

As for the distance from the edge *d*, only *NGasC*, *NMNC*, *NIMC* and *ONAM* show some level of correlation, which is negative in all cases.

Table 9. Correlation between input data and N-related model output variables. The colour gradient show where the value of each cell falls within the selected range, with red and green highlighting the strongest correlations (negative and positive).

	InNBal	OrgNBal	SNBAL	NIAD	NLCM	NGasC	NMNC	NIMC	LNTD	ONAM
TN	0.04	0.01	0.08	0.14	-0.09	0.04	0.41	0.50	0.08	0.23
SOC	0.29	0.02	0.30	0.19	-0.14	-0.04	0.60	0.67	0.33	0.38
pH	-0.21	-0.60	-0.41	-0.94	0.89	0.94	-0.85	-0.63	-0.36	0.74
Clay	-0.36	-0.52	-0.54	-0.84	0.88	0.90	-0.80	-0.57	-0.47	0.73
Sand	0.07	0.64	0.28	0.96	-0.95	-0.90	0.85	0.59	0.19	-0.83
Silt	0.11	-0.68	-0.11	-0.98	0.96	0.86	-0.83	-0.57	-0.01	0.85
d	0.00	0.05	0.00	0.05	-0.03	-0.27	-0.27	-0.33	-0.03	-0.44

InNBal, OrgNBal and SNBAL: Inorganic, organic, and seasonal N balance, NIAD: Total soil NO_{3^-} + NH_4^+, NLCM: N leached during season, NGasC: N Gas losses, NMNC: Cumulative N mineralization, NIMC: Cumulative N immobilization, LNTD: Total soil litter N, ONAM: Organic N at maturity, TN: total nitrogen, SOC: Soil organic carbon, d: distance from the forest edge, OCAM: Organic C at maturity.

The NIMC [kg ha^{-1}] (Figure 25, left) shows an important spatial variability across the field. As indicated by its inverse correlation to the distance d (-0.27), the NIMC increases at proximity to the forest edges. The same behaviour is observed for the ONAM [kg ha^{-1}], as shown in Figure 25 (right).

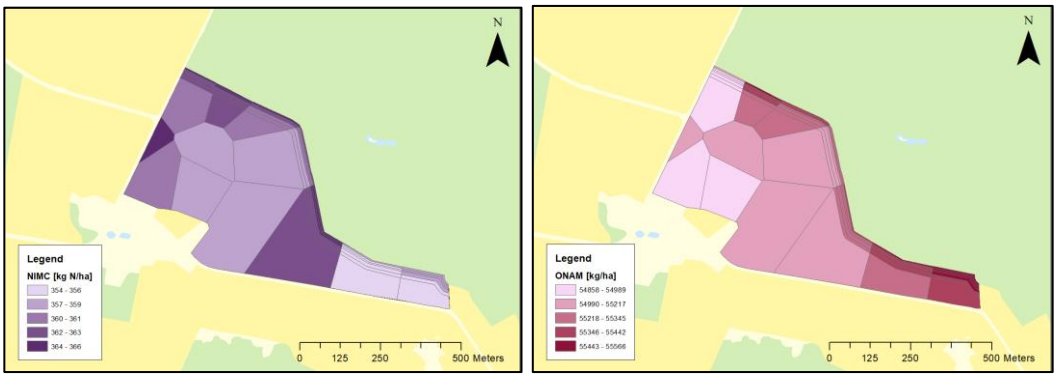

Figure 25. (Left) cartography of the cumulative N immobilization in kg ha^{-1} for year 2010 on studied site. (Right) cartography of the predicted organic nitrogen at maturity for year 2010 on studied site, Bjertorp, Kvänum, Sweden. Light to dark colours indicate a moderate to intense activity.

Table 10 indicates high correlations between N productivity and yield, especially for simulated yield. A high correlation was identified with the distance from the forest edges as well, indicating that the model was able to capture the distance effects.

Table 10. Correlation table regarding nitrogen productivity in relation to the distance to the forest edge (d) and the measured and simulated yield (HWAMM and HWAMS). The colour gradient show where the value of each cell falls within the selected range, with red and green highlighting the strongest correlations (negative and positive).

	Nitrogen productivity			
	DPNAM	DPNUM	YPNAM	YPNUM
TN	-0.39	0.29	-0.42	-0.26
d	0.73	-0.24	0.62	0.32
HWAMM	0.58	-0.38	0.61	0.46
HWAMS	0.83	-0.79	1.00	0.83

DPNAM: Dry matter-N fertilizer productivity [kg (DM)/kg (N fert)], DPNUM: Dry matter-N uptake productivity [kg (DM)/kg (N uptake)], YPNAM: Yield-N fertilizer productivity [kg (DM)/kg (N fert)], YPNUM: Yield-N uptake productivity [kg (DM)/kg (N uptake)].

The low correlation between TN initial observations and NMNC, NMIC and ONAM is illustrated by the lack of trend in Figure 26. The scatter plots do not follow a particular curve and are spread away from the 1:1 line. Normalized observations however show similar values highlighted by the apparition of vertical lines of points. This is probably due to the coarse resolution of the TN dataset that results in equal values for multiple polygons.

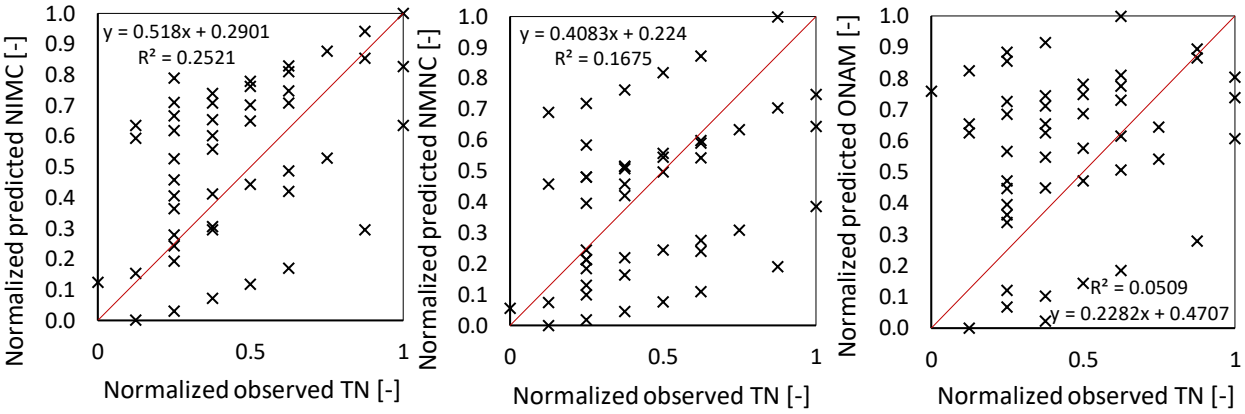

Figure 26. Normalized predicted (left) Cumulative Nitrogen immobilization (NIMC), (middle) Cumulative Nitrogen mineralization (NMNC), and (right) Organic Nitrogen at Maturity (ONAM) against normalized observed Total Nitrogen (TN).

4. Discussion

4.1 Methodological framework

The results showed that the methodological framework provides a good reference for the preparation of the different data modules needed to run the DSSAT models. The methodology was based on the best available data, mainly found in the literature (from open-source databases) or provided by SLU researchers. At the end, the simulation could be run with the files produced according to the steps described in the method section. The same method should be effective when applied to higher resolution data. There is indeed considerable room for improvement in the results obtained, for example by obtaining local data through the collection of soil samples instead of using gridded data. As the resolution of the soil data was rather coarse, Thiessen's method generated large polygons, which were considered homogeneous in terms of soil properties. Gridded data such as N data (500m resolution) leads to high uncertainties regarding such detailed effects as impacts of forest edges in individual fields. The availability of field samples would allow for a finer resolution and better accuracy in the predictions, given that soil heterogeneities arise from the small-scale distribution of chemical, physical and biological soil properties, substantially impacting water and nutrient retention capacity of individual soils (Wallor et al., 2018).

The SOC and TN concentration curves (Figure 20) could be more accurate if produced on the basis of site-specific soil data, providing SOC and TN concentrations at different distances from the forest edge.

In this study, the power trendlines were chosen as they provided the highest coefficient of determination (R^2). However, they bring important bias to the resulting SOC and TN concentrations. First, the concentrations tend to decrease infinitely as the distance increases, potentially resulting in unreasonably low concentrations at very large distances. Second, the functions show infinitely high concentrations at distances very close to 0m. In both cases, arbitrary decisions were necessary and the distances of 2.5 and 40 meters from the edges are assumed to be the limits. Furthermore, the data showed important variability with respect to the function. This is probably due to the combination of data from different studies, different locations, soil types or cropping systems. The paper from Schmidt et al.

(2017) provided most of the data, from replicates collected on the same sites thus adding in greater weight in the function than any other paper. Since most of the research has focused on the edges of hedgerows, tree lines or the inner side of forests adjacent to croplands, further research and data on forest edges is needed.

The distance from which SOC and TN concentrations are considered constant can be discussed. On-site measurements could be used to support the decision about the distance considered based on local soil properties and observations. It is also based on the hypothesis that the SOC and TN concentration decreases with distance from the forest, but soil samples could prove otherwise. This is reinforced by the fact that soil already shows in-field spatial heterogeneity without consideration of forest boundaries (Wallor et al., 2018).

As revealed by the correlation table in the result section (Table 5), several variables exhibit multicollinearity. Soil moisture contents (LL, DUL and SAT) show collinearity to soil pH and texture, cause by the use of pedotransfer equations (Equations 6, 7, 8 and 9). Similarly, bulk density and SOC content exhibit collinearity (r=-1), leading to a significant correlation between bulk density and distance. This phenomenon demonstrates the importance of independency between input variables and can be avoided if all data are collected at the site, making it unnecessary to use estimation equations for unknown variables (e.g., pedotransfer functions) (Wallor et al., 2018). Therefore, the correlations obtained between the variables would have more significance regarding the actual processes depicted by the model. Moreover, yield is more sensitive to certain variables, such as the available water capacity under rainfed conditions, leading to a significant difference in crop model outputs (Wallor et al., 2018). However, significant correlations were found, supporting the assumption that yield tends to decrease at smaller distances from the forest edges (inverse correlation to d), at the same time as increased concentrations in TN and SOC. One could relate these observations to crop N uptake as well as to carbon sequestration as processes occurring where crop growth is optimal. However, this would not be in line with the initial assumption that C and N concentrations are higher at the forest edge.

Soil moisture showed a low correlation with yields, suggesting that water availability is not a limiting factor for crop growth at the studied site. However, one should be careful with those observations due to the collinearity phenomenon described above.

As illustrated by the yield map (Figure 17) the Southern limit of the field showed a greater yield. That might reflect the typical Swedish sun radiations coming from the south and the interception of diffuse radiation from the trees on the Northern side.

Further research is needed to establish databases on the effects of forest edges on adjacent agricultural fields. This is essential to provide more data for the concentration functions to be created in the future, as well as for comparative research on the subject.

Other studies showed the importance of a better understanding of the soil heterogeneity at the field level. Site conditions and yield performance are shown to vary between polygons. Some authors proposed a field arrangement design based on “management zones" with adapted management practices that include specific soil and microclimatic properties (Wallor et al., 2018 ; Hernández-Ochoa et al., 2022). This would be in line with the use of different polygons such as in this study and it is a great example of application once forest borders effects are better understood.

Although the use of ArcMap is not always intuitive, it is an important complement for the visual evaluation of input and output variables, as well as for the preparation of soil data to be fed to DSSAT. However, the production of an alternative visual framework could also be considered for future work, as it gives the reader an overview of the steps ahead.

4.2 Model performance

The information obtained from DSSAT is recognised as a decision support tool for farmers and government for crop production optimisation and cropping system management (Hoogenboom et al., 2003). One drawback in the use of process-based models such as DSSAT is the characteristic of being a data-intensive model that combines a set of complex ecosystems. In addition, DSSAT is an old interface that has strongly been improved since the 1990’s but is sometimes unreliable to perform the tasks expected from it. Output files and codes are extremely numerous and complex. As an example, the TN did not appear in any of the output files. Furthermore, the simulation had to be run for each polygon individually to obtain the correct values regarding N allocation summary, increasing the amount of time required to run the simulations. Besides, DSSAT does not facilitate the conversion of units, as most of the output variables are expressed in kg ha^{-1}, whereas the initial N and SOC concentrations were imported as percentages.

Furthermore, the DSSAT crop models do not simulate horizontal fluxes, thus considering water re-distribution amongst polygons and surface runoff neglectable and therefore considerably simplifying natural processes (Buck-Sorlin, 2013).

In this study, the evaluation of the model is mixed. Although the index of agreement indicates a satisfactory fit between observed and predicted yields (*d-stat* = 0.662), and the NRMSE reflects a good prediction (NRMSE = 10.7%)

(Hoogenboom et al., 2003), the model evaluation showed poor model performance in accurately predicting in-field variability (R^2 = 0.36). The negative efficiency factor (EF < 0) suggests that significant improvements in data inputs are needed, indicating that P_i = M is a better approximation of the observed yield for the current simulation.

The crop growth and yield are impacted by an important number of factors, as illustrated by the many correlated variables to *HWAMM (*Table 7*)*. However, the differences highlighted by the table between the measured and simulated variables suggest that the model predictions are not able to properly depict all processes, as shown by some low or unmatched correlations.

However, if the simulation considered only the field core, the results would show a better agreement with the observed yield, as illustrated by the mapping of the prediction deviation (Figure 22 (left)). As illustrated by the Figure 21 and 22 (right), the model showed a tendency to overpredict yields, especially at the forest edge. The focus for improvement should therefore concentrate on polygons near forest edges.

Probably the major reason for this inability to accurately predict yield variability at the edges may be the lack of microclimatic data. Indeed, DSSAT was fed with uniform soil data, based on only 12 soil samples, although enhanced by a distance-adapted concentration of SOC and TN. Crucial processes such as light exposure, canopy interception, differential soil moisture and temperature related to the presence of trees at the edge of the field were left out. This information could be added by assessing microclimatic variations in various locations of the field. However, long-term, consistent, and robust data need to be collected and analysed (Schmidt et al., 2019). Microclimatic data could help to better depict the variability of growth, as it has important consequences on certain determining factors such as radiation and temperature (van Ittersum & Rabbinge, 1997). Microclimatic data can also have an impact on limiting factors such as soil moisture. This is therefore a crucial element to consider for future research.

Spatial soil heterogeneities at the field scale remain underexplored. Useful information could however be retrieved from such studies, by helping to understand how to exploit this heterogeneity in allocating crops. Hernández-Ochoa et al., (2022) suggest that management zones should be assigned with specific crop species or cultivar according to their soil properties/zone specification. As an example, high yielding crop cultivars could be grown on zones with optimum conditions, while more tolerant crops species could be grown on zones that show poor nutrient conditions or water availability. This approach is probably feasible for large areas, while for small fields the amount of work involved in changing seeds and adjusting the machinery might overcome the economic benefits. Some of

the poorest zones could hold biodiversity-improving species, flower strips or legumes, which could improve overall field productivity and ES provision. Landscape elements such as hedgerows and trees are also known for their beneficial effects on wind regulation and water erosion (Hernández-Ochoa et al., 2022).

Wallor et al. (2018) tested 11 different models to assess their sensitivity to soil variability and hydrological boundary conditions. The research supports the findings of this study on the need for more extensive data, indicating that the lack of information of subsoil properties could result in poor performance of all models. Interpolated and assumed values at unsampled depth had a significant impact on model performance. Data provided by Wallor et al. (2018) for a field in Germany would be worth assessing according to this study's methodological framework.

Hernández-Ochoa et al., 2022 outlined the importance of calibration, which should ideally be based on consistent and fine resolution data including multiple soil and crop state variables in parallel for several dates within one growing. Furthermore, the temporal replicates of samplings on a longer period could enable the calibration to be based on the 1st year of experiment, and provide more data from the 2nd and 3^{d} year for model validation as was proposed by Hernández-Ochoa et al. (2022) and Wallor et al. (2018).

4.3 Potentials and limitations for DSSAT to predict ecosystem services provision

In this study, it was expected that SOC, TN, and yield exhibit spatial heterogeneity at the forest edges due to differences in C input and decomposition rates of litter from trees (Bambrick et al., 2010).

4.3.1 Food production

With respect to the food production, the model tendency to overestimate the yield was already analysed above. Crop production depends on many different factors such as climate, soil characteristics, and crop species (Hai-long et al., 2017), with some factors more determining than others (van Ittersum & Rabbinge, 1997). It is not surprising that the DSSAT models were not able to consider all parameters with accuracy.

It is already remarkable that both the measured and predicted yield behave as expected with respect to the distance from the forest edge (highly positive correlation) (Table 7). However, it is important to keep in mind that the model was calibrated for that specific parameter, basing its estimations of genetic coefficients

on observed yield values. And whilst one could have expected some correlation coefficients to show similarities between the measured and predicted yield, it is surprising that both datasets still demonstrate strong correlations to different parameters.

Some correlation coefficients might show bias due to collinearity: this is the case for SOC, TN and d, as the latter was used to evaluate the increase in SOC and TN concentrations at the forest edge. In addition, pH and SOC parameters could be collinear because SOC was calculated from the SOM, and accumulation of soil organic matter through the decomposition process can lead to the increase of organic acids (Hong et al., 2019).

The negative correlation coefficient between yield and *NIAD* (NO_3^- + NH_4^+) at crop maturity suggests that plant uptake have occurred during crop growth, leaving less inorganic N available for the plants behind. It is a bit unclear what the organic and inorganic N balances represent, especially because they show correlations coefficient that do not match those of *ONAM* and *NIAD*, respectively. Besides, while the Organic N balance shows a significantly negative correlation to measured yield, inorganic N coefficient is neglectable. On the other hand, the Inorganic N balance shows a strong positive correlation with predicted yield. The lack of correlation between both yield datasets and *ONAM* could be explained by the fact that the N uptake does not matter anymore at maturity. It seems like other variables could be more explanatory about the loss of N, however, such as *NLCM* and inorganic N, due to the high mobility of NO_3^- in soil.

At last, it is interesting to note that N_2O and CO_2 gaseous losses are positively correlated to simulated yield. These results support the assumption that the provision of food balances with other ES such as climate mitigation and air quality, as increased yields tend to occur along greater gas emissions.

For a better understanding of the overall behaviour of the system, it would be important to determine the correlation with meteorological data.

When it comes to yield data, it is challenging to look at field edge effect, due to the presence of artefacts in the yield data. And while it is crucial to filter the data to identify any outliers, this often results in a loss of detail on the variability that one might be trying to assess. The yield map (Figure 17) depicts the greatest variability in the data. However, it can be biased especially on the edges due to practical harvesting. While harvest usually starts from the edges (to open space for the combine to turn later), the yield scale installed in the combine sensors is operating at all times meaning that when it is turning on an empty area it still registers weight. As a result, edges are always more compacted due to heavy machinery traffic (Carlesso et al., 2019), which is one of the possible explanations for lower yield on the upper left edge of the field (Figure 21 (right)). In addition, the observed yield

data have been averaged, thus losing some of their variability, resulting in more uniform values.

Information on the current and historical use of the field and its surroundings could also provide an explanation for the observed spatial variability in yield. In 2010, the field was adjacent to a road to the west and to a household in the lower left corner. Shade and cardinal direction are also factors that can affect crop yields, through differential solar radiation, as discussed with van Ittersum & Rabbinge (1997) founding.

Besides, forests are also known to have effects on local microclimatic parameters such as wind speed, soil moisture, and light incidence, which can lead to changes in water, nutrient absorption, and photosynthesis.

4.3.2 Carbon sequestration

SOC is affected by many factors, such as crop yield, temperature, and microbiological activity. As a cropping system model, DSSAT cannot simulate all those factors (Hai-long et al., 2017). Nevertheless, the model still predicts relatively accurate values and variability for the SOC at maturity. The correlation between predicted and observed SOC is particularly high, with a small tendency to overpredictions. This suggests that the model potentially predicts a long-term SOC accumulation, which would support the assumption that forest edges positively affect carbon sequestration, as shown by the Figure 24. This is also indicated by SOC's correlation with the distance to the forest (d=-0.56), which is observed for the *OCAM* as well (d=-0.63). *OCAM* is significantly correlated to soil pH, which suggests that pH is responsible for chemical processes regarding C compounds in the soil, especially inorganic C. Organic matter can also affect soil pH through the accumulation of organic acids (Hong et al., 2019).

Surprisingly, *HWAMS* is not as much correlated to SOC and *OCAM* (r=-0.03 and r=-0.16) than *HWAMM* is (r=-0.49 and -0.54). It seems like the model did not depict accurately the correlation between yield and SOC/*OCAM*. However, the correlations between yield (measured and simulated) and cumulative CO_2 emissions from soil (CO2EC) are both significant, suggesting a better ability of the model to estimate gaseous emissions from the C cycle (Figure 3).

4.3.3 Nitrogen retention

The poor fit between observed TN and N-related output variable demonstrates the failure of the model to accurately explain the fate of N. However, the N cycle is complex cycle with various inputs and outputs that are hard to quantify (Figure 4). Moreover, DSSAT does not take runoff and horizontal fluxes into account, omitting a potentially important output pathway of N. Although it was expected that forest

edges reduce N leaching and losses by having more organically bound N, *NLCM* does not show any significant correlation with distance from the forest.

Overall, simulated variables show a high correlation to soil texture, in particular for *NIAD* and *NLCM*. This might reflect the great retention potential of negatively charged clay particles, to which NH_4^+ is easily bound to. In basic environments, NH_4^+ liberates an H^+ to volatilize as NH_3 (Brennan, 2022).

Basic pH soils might exhibit less N leaching, as indicated by the positive correlation of *NLCM* to pH.

It is surprising that both cumulative mineralization and immobilization show a significant correlation to the distance from the forest, suggesting a more intense N cycling at the forest edge. It might be related to the concentrations of TN that increase at the edges, to which both variables are positively correlated too (potential for collinearity).

The N productivity (Table 10) is well correlated to the distance from the forest edge, indicating the better ability of the crop to make use of the N at the centre of the field, where the yield is relatively higher. These results support this study's assumption that the areas close to the forest show trade-offs between provisioning (food supply) and supporting ES (N retention).

The N retention is regulated by complex processes such as particle binding, crop uptake, immobilization, mineralisation and denitrification. It is hard to depict clear trends from the results obtained, especially in a fertilized field, considering the significant artificial input of N. Furthermore, specific variables such as seasonal TN were not provided by the model for the entire soil depth, which appears surprising for such a decision support tool. Besides, the processes regarding the N fate seem to have a stronger correlation to other input variables than TN. A variable that identifies the C:N ratio would be of great interest as well, as an indicator of soil quality.

Many variables were computed for daily output, which represented to much averaging and sorting work to assess for this project's scope. Again, the lack of microclimatic data might explain the poor model performance regarding N predictions, resulting in a lack of clear trend between measured and simulated variables (Figure 26).

One can add that the model had difficulty in including the initial TN values in the simulation, even involving running it several times and for each polygon individually. It is still not obvious if the model took the TN into account in its calculation. With the use of DSSAT crop models, other indicators than the TN should be considered due to the difficulty to find an equivalent in the output

variables. Organic nitrogen at maturity (*ONAM*) or total soil NO_3^- + NH_4^+ (*NIAD*) could be considered.

4.3.4 General remarks

All the processes occurring in the soil and within the plant and atmosphere are heavily intertwined (Gruber & Galloway, 2008). They are highly determined by local environment such as chemical and soil properties like pH and soil texture, hydrology and microclimate. The extreme complexity of such processes cannot be encapsulated by a model, even if agro-ecosystem models are getting better at depicting interactions and correlations between the multiple parameters and compounds at stake. Furthermore, all feedbacks resulting from changes in the natural nutrient cycles are balanced and can vary depending on site-specific characteristics, as mentioned above (van Ittersum & Rabbinge, 1997; Hernández-Ochoa et al., 2022). This increases the uncertainties related to CS modellisation.

Besides, a strong correlation between two variables is not a proof of causality, and even though the soil-plant atmosphere system is at heart of many well-documented processes, there are still uncertainties about how to quantify those processes. Collinearity can also be a source of bias in the interpretation of the interaction of different variables.

Propositions for improvements and future assessments include control samples at all field edges to allow for a comparison between forested and non-forested edges. It seems that the yield map showed lower yield at proximity to most borders (Figure 17). This could result from a greater soil compaction from heavy machinery.

A future experimental design should include several soil samples and replicates to be collected in the field, at given distances from the forest and various depth. The data collected should encompass the exact location of the sample, as well as the soil properties and chosen indicators.

More refined, field-specific and higher resolution observations would probably improve the understanding between variables correlations and lead to more precise effects resulting from soil heterogeneity, as the aim in the long run would be for the model to depict spatial variation at smaller scale (Hernández-Ochoa et al., 2022).

Until now, agriculture has focused on increasing yields to the greatest extent at the expense of the environment, with considerable damage to soil, water, and air quality. Intensive production succeeded through the spread of intensive agricultural systems that left no room for natural habitats and biodiversity.

Carbon sequestration and nitrogen retention lie amongst a wide range of ES to promote through the CS management strategies that would make the food system

more resilient. Many strategies that include crop and landscape diversification have been proved to increase the provision of such ES (e.g., intercropping, flower strips, hedgerows, etc.) (Bambrick et al., 2010; De Stefano & Jacobson, 2018; Alberti et al., 2021). Therefore, field division in management zones, as suggested by Hernández-Ochoa et al. (2022), could lead to a more efficient use of the landscape and its soil characteristics. Smaller patches would allow for the allocation of specific crops and objectives, focusing on particular ES depending on their specific location. Non-edible crops that benefit biodiversity and ES could be placed with a better understanding of nutrients and water cycles in order to improve overall productivity and allow for the food system to be more sustainable.

Depending on the ES to be enhanced, the optimal size of fields and the importance of forest edges vary. As illustrated in Figure 7, the future of cropping systems lies in promoting the multifunctionality found in natural ecosystems. Although food production is essential for global food security, it must be supplemented by other (supporting) ES that will ensure resilient and sustainable food supply in the long term.

Machinery size and labour costs are currently a limiting factor that hinders the reduction of field sizes. But it is hoped that the development of new technologies will provide better tools to enable the redefinition of the scale of zoning management (Hernández-Ochoa et al., 2022)

Finally, the transition to multifunctional cropping systems must be accompanied by policy adjustments to enable a change in consumption and societal behaviour, including through taxation and heavy regulatory tools. Agricultural expansion is driven by market pressure and cannot be stopped by the mere will of farmers or scientists.

The implementation of sustainable and environmentally friendly farming systems seems to be one of the many measures needed to ensure a sustainable food production system and is in line with the European objective aimed at promoting small farms, in order to preserve local traditions and products (Eulalia Claros, 2014). Smaller fields are thought to be associated with a wider range of ES, particularly for biodiversity and species richness (habitat use and complementary resources at the boundaries) and risk control (e.g., pests and diseases, flooding, and yield losses) (Hernández-Ochoa et al., 2022). The Common Agricultural Policy has recently increased European Green Deal's ambitions with financial support for farmers who adopt climate-sensitive and nature-friendly practices despite trade-offs on food production and thus yield (European Union, 2022; Hernández-Ochoa et al., 2022).

Research such as this one could provide a reference for discussions between policy makers, farmers, and researchers to address the current challenges posed by agriculture and its associated landscape fragmentation.

5. Conclusion

This research achieved its objective of providing a methodological framework for the assessment of ecosystem services with DSSAT crop models. Using the best available data, this study was a first attempt to describe the spatial variability of yield, SOC and TN in the vicinity of forest edges at the field scale. It highlighted several limitations, such as the lack of high-quality datasets concerning the microclimate associated with forest edges, the poor quality of gridded data, thus underlining the importance of site-specific data collection.

The analysis of the results demonstrated the bias induced by the potential collinearity between some variables, leading to misinterpretations.

Few other studies of soil heterogeneities in the field were found, demonstrating the need for further research on this topic, especially in heterogeneous landscapes that include forests or other structural elements.

As for model performance, the results of this study were encouraging. They already showed room for improvement with regard to the production of high-quality datasets. Whilst DSSAT performed a reasonable prediction for yield, it bared a bias that could partially be corrected by recalibration using microclimatic data, that emphasise the differences in potential production by providing differential defining factors. Process-oriented, dynamic agro-ecosystem models such as DSSAT could offer an appropriate tool for assessing soil heterogeneity in the future, in particular at the forest edges, and the consequences for the provision of ecosystem service.

In summary, there is great potential for the assessment and promotion of more multifunctional cropping systems. There is a growing demand for the transition to climate and environmentally sensitive farming practices, which require policy support to offset the trade-offs in food production.

There are still many variables to be examined due to the large amount of data, processes and results produced by DSSAT, and crop models in general. These elements go beyond the scope of this research but are certainly worth further study.

References

Aggarwal, P. et al., 2001. *Land use analysis and planning for sustainable food security: with an illustration for the state of Haryana, India.* s.l.:New Delhi: Indian Agricultural Research Institute; Los Baños: International Rice Research Institute; Wageningen: Wageningen University and Research Centre.

Alberti, P., Becker, T., Jones, J. & Johanning, N., 2021. Chapter 5: Cropping Systems and Alternative Crops. Dans: U. o. Illinois, éd. *Illinois Agronomy Handbook.* Urbana-Champaign: s.n., pp. 1-32.

Alderman, P., 2021. *DSSAT: A Comprehensive R Interface for the DSSAT Cropping Systems Model. R package version 0.0.6.* [Online] Available at: https://CRAN.R-project.org/package=DSSAT

Altieri, M. A., Nicholls, C. I., Henao, A. & Lana, M. A., 2015. Agroecology and the design of climate change-resilient. *Agronomy for Sustainable Development*, Volume 35, pp. 869-890.

Ballabio, C. et al., 2019. Mapping LUCAS topsoil chemical properties at European scale using Gaussian process regression. *Geoderma,* 355(113912).

Bambrick, A. D. et al., 2010. Spatial heterogeneity of soil organic carbon in tree-based intercropping systems in Quebec and Ontario, Canada. *Agroforestry Systems,* Volume 79, pp. 343-353.

Berazneva, J. et al., 2019. Agricultural Productivity and Soil Carbon Dynamics: A Bioeconomic Model. *American Journal of Agricultural Economics*, Volume 101, pp. 1021-1046.

Bergkvist, G. et al., 2015. *The SLU road map for cropping/forestry system research*, Uppsala: SLU.

Beven, K. & Freer, J., 2001. Equifinality, data assimilation, and uncertainty estimation in mechanistic modelling of complex environmental systems using the GLUE methodology. *Journal of Hydrology,* pp. 11-29.

Boote, K., 1999. *Concepts for calibrating crop growth models. DSSAT version, 3.* s.l.:s.n.

Boote, K., 2019. *Advances in crop modelling for a sustainable agriculture.* London: Burleigh Dodds Science Publishing.

Brennan, R., 2022. Chemical amendment of dairy cattle slurry for the control of phosphorus in runoff from grassland.

Buck-Sorlin, G., 2013. Process-based Model. Dans: *Encyclopedia of Systems Biology.* New York: Springer, p. 1755.

Burras, L. et al., 2001. Carbon Sequestration: Position of the Soil Science Society of America. *Soil Science Society of America,* Volume 65, pp. 1-4.

Carlesso, L. et al., 2019. Soil compaction effects on litter decomposition in an arable field: Implications for management of crop residues and headlands. *Applied Soil Ecology,* pp. 31-37.

Carpenter, S. R., Bennett, E. M. & Peterson, G. D., 2006. Scenarios for Ecosystem Services: An Overview. *Ecology and Society,* 11(29).

Chapin, F. S. et al., 2009. The changing global carbon cycle: linking plant–soil carbon dynamics to global consequences. *Journal of Ecology,* Volume 97, pp. 840-850.

Chisanga, C. B., Phiri, E., Shepande, C. & Sichingabula, H., 2015. Evaluating CERES-Maize Model Using Planting Dates and Nitrogen Fertilizer in Zambia. *Journal of Agricultural Science,* 7(3).

Corning, E., Sadeghpour, A., Ketterings, Q. & Czymmek, K., 2016. *The Carbon Cycle and Soil Organic Carbon,* s.l.: Cornell University's College of Agriculture and Life Sciences .

Creutzig, F. et al., 2022. Chapter 5: Demand, services and social aspects of mitigation.. Dans: *limate Change 2022: Mitigation of Climate Change. Contribution of Working Group III to the Sixth Assessment Report of the Intergovernmental Panel on Climate Change* . Cambridge, UK and New York: Cambridge University Press.

D'Acunto, L., Semmartin, M. & M.Ghersa, C., 2014. Uncropped field margins to mitigate soil carbon losses in agricultural. *Agriculture, Ecosystems and Environment,* Volume 183, pp. 60-68.

D'Acunto, L., Semmartin, M. & Ghersa, C. M., 2016. Uncultivated margins are source of soil microbial diversity in an. *Agriculture, Ecosystems and Environment,* Volume 220, pp. 1-7.

De Stefano, A. & Jacobson, M. G., 2018. Soil carbon sequestration in agroforestry systems:. *Agroforestry Systems,* Volume 92, p. 285–299.

Developers, Google, 2022. *Normalization.* [Online] Available at: https://developers.google.com/machine-learning/data-prep/transform/normalization?hl=en

Drexler, S., Gensior, A. & Don, A., 2021. Carbon sequestration in hedgerow biomass and soil in the temperate climate zone. *Regional Environmental Change,* 21(74).

Eckersten, H., 2017. *Cropping system research - A framework based on a literature review,* Uppsala: Swedish University of Agricultural Sciences (SLU).

EPA, 2022. *Inventory of U.S. Greenhouse Gas Emissions and Sinks: 1990-2020,* s.l.: U.S. Environmental Protection Agency.

ESDAC, 2019. *European Commission, Joint Research Center.* [Online] Available at: https://esdac.jrc.ec.europa.eu/content/chemical-properties-european-scale-based-lucas-topsoil-data#tabs-0-description=0 [Accessed 9 September 2022].

Eulalia Claros, M. S., 2014. *European Parliament Research Service.* [Online] Available at: europarl.europa.eu/RegData/bibliotheque/stspotlight/2014/140794/LDM_STS(2014)140794_REV1_EN.pdf [Accessed 24 November 2022].

European Union, 2022. *Infographic - A fairer, greener and more performance based EU agricultural policy.* [Online] Available at: https://www.consilium.europa.eu/en/infographics/cap-reform/

Fahrig, L., 2003. Effects of Habitat Fragmentation on Biodiversity. *Annual Review of Ecology, Evolution, and Systematics,* 34(1), pp. 487-515.

FAO, 2015. *Agroforestry.* [Online] Available at: https://www.fao.org/forestry/agroforestry/80338/en/ [Accessed 7 September 2022].

Fischer, G., Shah, M., Tubiello, F. & Van Velhuizen, H., 2005. Socio-economic and climate change impacts on agriculture: an integrated assessment, 1990–2080. *Philos Trans R Soc Lond B Biol Sci,* 360(1463), p. 2067–2083..

Foley, J. A. et al., 2005. Global Consequences of Land Use. *Science,* 309(570).

Gikas, G. D., Tsihrintzis, V. A. & Sykas, D., 2016. Effect of trees on the reduction of nutrient concentrations in the soils of cultivated areas. *Environmental Monitoring and Assessment,* 188(327).

Groenendyk, D., Ferré, T., Thorp, K. & Rice, A., 2022. Hydrologic-Process-Based Soil Texture Classifications for Improved Visualization of Landscape Function. *Plos One.*

Gruber, N. & Galloway, J. N., 2008. An Earth-system perspective of the global nitrogen cycle. *Year of the planet Earth.*

Gutzler, C. et al., 2015. Agricultural land use changes - a scenario-based sustainability impact assessment for Brandenburg, Germany. *Ecological Indicators,* pp. 505-517.

Hai-long, L. et al., 2017. Using the DSSAT model to simulate wheat yield and soil organic carbon under a wheat-maize cropping system in the North China Plain. *Journal of Integrative Agriculture,* 16(10), pp. 2300-2307.

Haynes, R. J., 1986. *Mineral Nitrogen In The Plant-Soil System.* Orlando: Academic Press.

He, J., Jones, J. W., Graham, W. D. & Dukes, M. D., 2010. Influence of likelihood function choice for estimating crop model parameters using the generalized likelihood uncertainty estimation method. *Agricultural Systems,* 103(5), pp. 256-264.

Hernández-Ochoa, I. M. et al., 2022. Model-based design of crop diversification through new field arrangements in spatially heterogeneous landscapes. A review. *Agronomy for Sustainable Development,* pp. 42-74.

Hong, S., Gan, P. & Chen, A., 2019. Environmental controls on soil pH in planted forest and its response to nitrogen deposition. *Environmental Research,* pp. 159-165.

Hoogenboom, G. et al., 2003. *Decision Support System for Agrotechnology Transfer Version 4.0.* Honolulu, HI: University of Hawaii.

Hoogenboom, G. et al., 2019. The DSSAT crop modeling ecosystem. Dans: *Advances in Crop Modeling for a Sustainable Agriculture.* Cambridge: Burleigh Dodds Science Publishing, pp. 173-216.

Hoogenboom, G. et al., 2021. *Decision Support System for Agrotechnology Transfer (DSSAT) Version 4.8 (DSSAT.net),* Gainesville: s.n.

ICOS, n.d. *Lanna.* [Online] Available at: https://www.icos-sweden.se/Lanna [Accessed 20 September 2022].

IPCC, 2022. *Climate Change 2022: Impacts, Adaptation and Vulnerability,* Cambridge: Cambridge University Press.

Jansson, C. et al., 2021. Crops for Carbon Farming. *Frontiers in Plant Science,* Volume 12.

Johnson, C. et al., 2005. Nitrogen Basics – The Nitrogen Cycle. *Cornell University's College of Agriculture and Life Sciences.*

Jones, J. et al., 2003. DSSAT Cropping System Model. *European Journal of Agronomy,* Volume 18, pp. 235-265.

Kätterer, T., Andrén, O. & Jansson, P.-E., 2006. Pedotransfer functions for estimating plant available water and bulk density in Swedish agricultural soils. *Acta Agriculturae Scandinavica, Section B - Soil and Plant Science* , 56(4), pp. 263-276.

Knoll, A. H., Canfield, D. E. & Konhauser, K. O., 2012. The Global Nitrogen Cycle. Dans: *Fundamentals of Geobiology.* Oxford: Wiley, pp. 36-48.

Kramer, K. et al., 2022. Roadmap to develop a stress test for forest ecosystem services supply. *One Earth,* pp. 25-34.

Kuemmel, B., 2003. Theoretical investigation of the effects of field margin and hedges on crop yields. *Agriculture, Ecosystems and Environment,* Volume 95, pp. 387-392.

Lal, R., Kimble, J. M., Follett, R. F. & Stewart, B., 2018. *Soil Processes and the Carbon Cycle.* s.l.:CRC Press.

Malézieux, E., 2012. Designing cropping systems from nature. *Agronomy for Sustainable Development,* Volume 32, pp. 15-29.
Mayer, D. & Butler, D., 1993. Statistical validation. *Ecological Modelling,* pp. 21-31.
McClaugherty, C., 2001. Soils and Decomposition. *ENCYCLOPEDIA OF LIFE SCIENCES,* pp. 1-8.
McMeekin, N., Wu, O., Germeni, E. & Briggs, A., 2020. How methodological frameworks are being developed: evidence from a scoping review. *BMC Medical Research Methodology,* 20(173), pp. 1-9.
McMeekin, N., Wu, O., Germeni, E. & Briggs, A., 2020. How methodological frameworks are being developed: evidence from a scoping review. *BMC Medical Research Methodology,* 20(173), pp. 1-9.
Millennium Ecosystem Assessment, 2005. *Ecosystems and Human Well-being: Synthesis,* Washington, DC: Island Press.
Mitchell, M. G. E., Bennett, E. M. & Gonzalez, A., 2014. Forest fragments modulate the provision of multiple ecosystem services. *Journal of Applied Ecology,* Volume 51, p. 909–918.
Mitchell, M. G. et al., 2015. Landscape Fragmentation and Ecosystem Services: A Reply to Andrieu et al.. *Trends in Ecology & Evolution,* 30(11), pp. 634-635.
Mitchell, M. G. et al., 2015. Reframing landscape fragmentation's effects on ecosystem services. *Trends in Ecology & Evolution,* 30(4), pp. 1-9.
NASA Langely Research Center, n.d. *Power Data access viewer.* [Online] Available at: https://power.larc.nasa.gov/data-access-viewer/
NASA, 2011. *The Carbon Cycle.* [Online] Available at: https://earthobservatory.nasa.gov/features/CarbonCycle [Accessed 6 September 2022].
Nations, U., 2018. SDG 7. *Science.*
Pardon, P. et al., 2017. Trees increase soil organic carbon and nutrient availability in temperate agroforestry systems. *Agriculture, Ecosystems and Environment,* Volume 247, pp. 98-111.
Pereira, H. M. et al., 2005. Condition and trends of ecosystem services and biodiversity. *Ecosystems and human well-being: multi scale assessments,* Volume 4, p. 171–203.
Piikki, K. & Söderström, M., 2019. Digital soil mapping of arable land in Sweden – Validation of performance at multiple scales. *Geodermaa,* Volume 352, pp. 342-350.
Rabbinge, R., 1993. The ecological background of food production. Dans: *Crop Protection and Sustainable Agriculture.* Chichester, UK: Wiley, pp. 2-29.
Rodríguez, J. P. et al., 2006. Trade-offs across Space, Time, and Ecosystem Services. *Ecology & Society,* 11(1).
RStudio Team, 2022. *RStudio: Integrated Development for R,* Boston: s.n.
Santoro, A., Venturi, M., Bertani, R. & Agnoletti, M., 2020. A Review of the Role of Forests and Agroforestry Systems in the FAO Globally Important Agricultural Heritage Systems (GIAHS) Programme. *Forests,* 11(860), pp. 1-21.
Sarkar, R., 2009. Use of DSSAT to model cropping systems. *CABI Reviews.*
Schmidt, M., Jochheim, H., Kersebaum, K.-C. & Lischeid, G., 2017. Gradients of microclimate, carbon and nitrogen in transition zones of. *Agricultural and Forest Meteorology,* Volume 232, pp. 659-671.
Schmidt, M., Lischeid, G. & Nendel, C., 2019. Microclimate and matter dynamics in transition zones of forest to arable land. *Agricultural and Forest Meteorology,* Volume 268, pp. 1-10.
Schumann, A., 1998. Thiessen polygon. *Encyclopedia of Hydrology and Lakes,* p. 648–649.

SGU, 2022. *Lerhaltskartan - digital åkermarkskarta.* [Online] Available at: https://www.sgu.se/samhallsplanering/planering-och-markanvandning/markanvandning/jordbruk-skog-och-fiske/lerhaltskartan-digital-akermarkskarta/

SLU, 2022. *Lanna research station.* [Online] Available at: https://www.slu.se/en/departments/soil-environment/field-stations/lanna/ [Accessed 20 September 2022].

SLU, 2022. *Weather stations.* [Online] Available at: https://www.slu.se/en/faculties/nj/this-is-the-nj-faculty/collaborative-centres-and-major-research-platforms/faltforsk-field-research-unit/weather/weather-stations/

SLU, n.d. *SLU.GET.* [Online] Available at: https://zeus.slu.se/get/?drop= [Accessed 14 September 2022].

SMHI, n.d. *SLU - Weather Data.* [Online] Available at: http://www.ffe.slu.se/lm/LMHome.cfm?LMSUB=0&ADM=0 [Accessed 16 September 2022].

Söderström, M., Sohlenius, G., Rodhe, L. & Piikki, K., 2016. Adaptation of regional digital soil mapping for precision agriculture. *Precision Agriculture,* Volume 17, pp. 588-607.

Soler, C. M. T., Sentelhas, P. C. & Hoogenboom, G., 2007. Application of the CSM-CERES-Maize model for planting date evaluation and yield forecasting for maize grown off-season in a subtropical environment. *European Journal of Agronomy,* pp. 165-177.

Torralba, M. et al., 2016. Do European agroforestry systems enhance biodiversity and ecosystem services? A meta-analysis. *Agriculture, Ecosystems & Environment,* Volume 230, pp. 150-161.

Tovihoudji, P. G., Akponikpè, P. B. I., Agbossou, E. K. & Bielders, C. L., 2006. Using the DSSAT Model to Support Decision Making Regarding Fertilizer Microdosing for Maize Production in the Sub-humid Region of Benin. *Frontiers in Environmental Science.*

USDA, 2011. *Carbon to Nitrogen Ratios in Cropping Systems,* s.l.: s.n.

van Ittersum, M. & Rabbinge, R., 1997. Concepts in production ecology for analysis and quantification of agricultural input-output combinations. *Field Crops Research,* pp. 197-208.

Van Vooren, L. et al., 2018. Monitoring the Impact of Hedgerows and Grass Strips on the Performance of Multiple Ecosystem Service Indicators. *Environmental Management,* Volume 62, pp. 241-259.

Viaud, V. & Kunnemann, T., 2021. Additional soil organic carbon stocks in hedgerows in crop-livestock areas. *Agriculture, Ecosystems and Environment,* 305(107174).

WA Government, 2022. *Agriculture and Food - Government of Western Australia.* [Online] Available at: https://www.agric.wa.gov.au/measuring-and-assessing-soils/what-soil-organic-carbon [Accessed 12 September 2022].

Wallach, D., Makowski, D., Jones, J. W. & Brun, F., 2019. *Working with Dynamic Crop Models: Methods, Tools and Examples for Agriculture and Environment.* s.l.:Academic Press.

Wallor, E. et al., 2018. The response of process-based agro-ecosystem models to within-field variability in site conditions. *Field Crops Research,* pp. 1-19.

You, L. & Sun, Z., 2022. Mapping global cropping system: Challenges, opportunities, and future perspectives. *Crop and Environment,* Volume 1, pp. 68-73.

Popular science summary

In recent years, agricultural land-use planning has become a central issue regarding both food security and climate change mitigation. Agriculture has always determined the configuration of the landscape in order to optimize yield, machinery use and monetary benefits. And while food production was once the primary objective of agricultural activities, it is now clear that compromises must be made. Today, agricultural land is seen as having promising potential for climate regulation and biodiversity, as well as for the restoration of natural areas. However, recovering these benefits from cropland requires changes from conventional agricultural practices.

In nature, trees play a crucial role in biodiversity, soil formation, the water cycle and climate change mitigation. Because of agriculture, trees have given way to hectares of arable land for cultivation. However, alternative designs that include incorporating trees within agricultural land could improve overall yields while ensuring the long-term ability of land to provide food and withstand sudden natural hazards. Trees could play a major role in restoring many of the natural benefits that agricultural lands can no longer provide. Previous publications have highlighted some tree-induced trends in soil carbon storage (reducing greenhouse gases in the atmosphere) and nitrogen retention (preventing water and soil pollution). Evaluated at the field scale, the benefits of integrating trees into agricultural fields could provide useful expertise to farmers and policy makers regarding the landscape configuration to be promoted for environmental preservation and protection.

In this Master Thesis, three objectives were pursued:

First, it was aimed to propose a procedure for evaluating the selected benefits observed near forest edges for a field in Bjertorp, Sweden. This was a first attempt to use a crop model to describe the spatial variability of an agricultural field with respect to yield, soil carbon and nitrogen concentrations as indicators of the impacts of trees on food production, carbon storage and nutrient cycling (mitigation and regulation benefits).

Second, the ability of the crop model to predict this spatial variability of the selected indicators was assessed. To do this, observed yield data from the study site were compared to simulated yield data produced by the crop model. The model was

based on a set of initial data on soil and weather conditions to provide a simulation as close to reality as possible.

Third, the potential and limitations of using the crop model were highlighted and discussed for possible improvements as well as for developing future research on forest edges along agricultural fields.

The results showed encouraging results regarding the use of the crop model to predict the spatial variability of selected benefits associated with the presence of trees, especially in the central area of the field. However, predictions near forest edges could be improved by using local climate data that are known to have a major impact on soil properties, local temperatures, and thus yield. The predictions of carbon and nitrogen concentrations have some bias at the forest edge due to the inability of the model to accurately predict yield and technical limitations of the crop model (interface, "old" model, ungenerated variables...).

High-quality data on both microclimate and site-specific soil properties are needed for further research to obtain more detailed results regarding spatial variability in yield and other natural benefits. This could help shape future policies in promoting more sustainable agriculture, especially through appropriate landscape organization.

THE BENEFITS RETRIEVED FROM FORESTED EDGES ALONG CROPLANDS

TRADE-OFF BETWEEN FOOD PRODUCTION AND OTHER NATURAL BENEFITS BROUGHT BY TREES

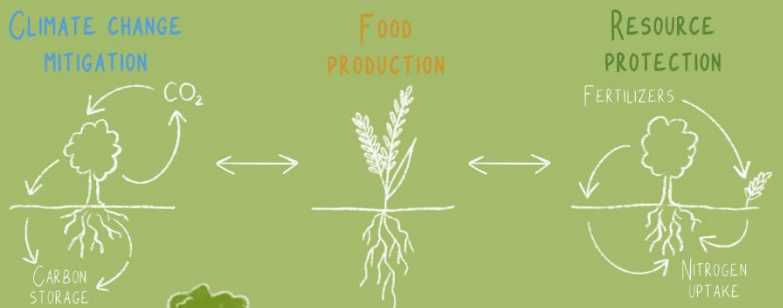

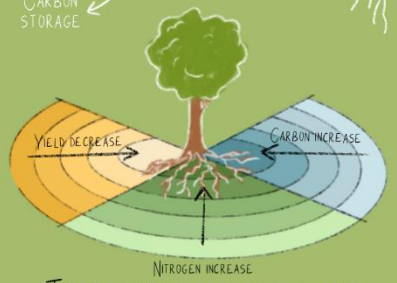

TREES INDUCE SPATIAL VARIABILITY WITHIN A SINGLE FIELD

3 INDICATORS :

YIELD FOR FOOD PRODUCTION
CARBON FOR CLIMATE MITIGATION
NITROGEN FOR RESOURCE PROTECTION

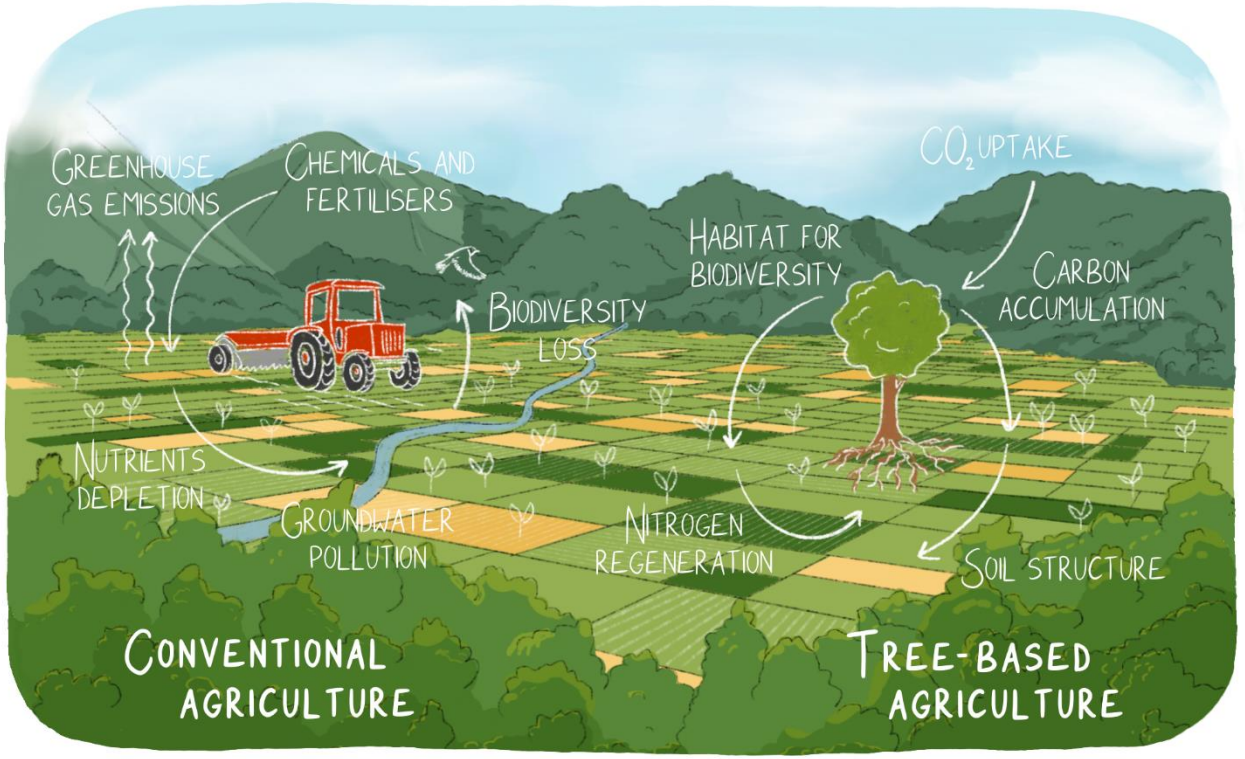

METHODOLOGICAL PROCEDURE

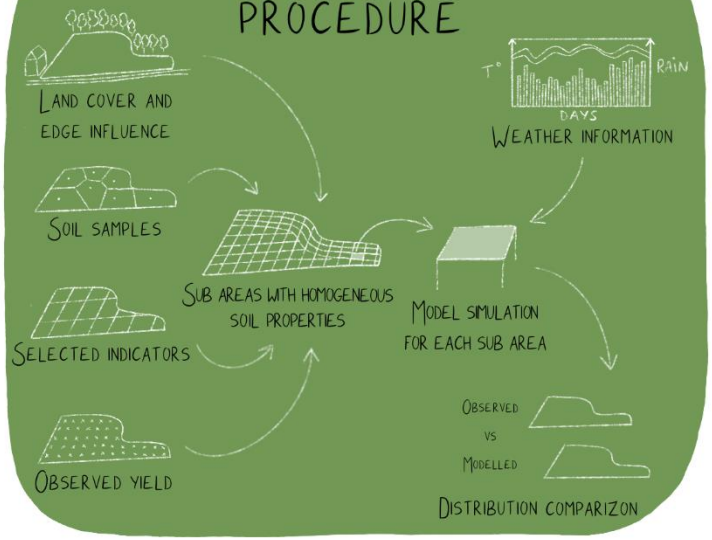

MODEL EVALUATION

ACCURATE PREDICTIONS FOR AREAS LOCATED FAR FROM THE FORESTED EDGES

PREDICTION OF A SLIGHT CARBON ACCUMULATION

FAILURE TO PREDICT NITROGEN FATE

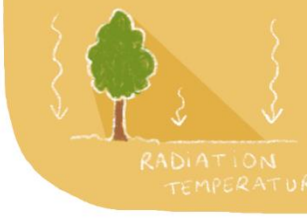

OVERALL OVERPREDICTION, INCREASED AT THE FOREST EDGES

→ MICRO LOCAL WEATHER CONDITIONS COULD IMPROVE THE PREDICTIONS

POTENTIAL AND LIMITATIONS

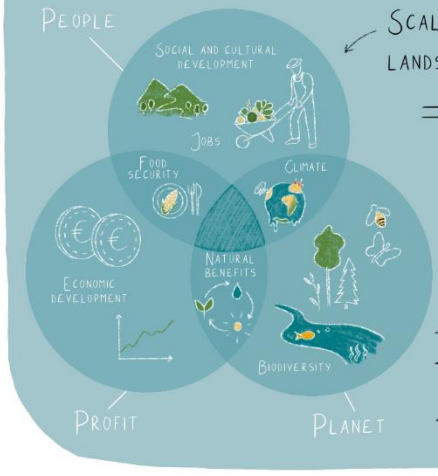

SCALE UP AT THE LANDSCAPE LEVEL

= TOOL FOR DECISION MAKER

FUTURE RESEARCH SHOULD COPE WITH :

- SITE SPECIFIC DATA
- HORIZONTAL FLOWS BETWEEN SUB AREAS
- MODEL LIMITATIONS

AUTHOR, CONCEPTION AND ILLUSTRATION: JULIETTE NGUYEN

Acknowledgements

I would like to express my gratitude to Bjertorp farm (Lantmännen) for providing soil information and yield data that allowed the model calibration. I owe thanks to Johanna Wetterlind (Soil and Environment department, SLU) for selecting fields and preparing the data for analysis.

I also want to thank my supervisors Marcos Lana and Henrik Meilby for their precious help along my research. I would like to address a special thanks to Marcos Lana for providing the research topic and for his daily help and support. Marcos also took care of the model's calibration, for which I am grateful.

Appendix 1: R code to generate soil profiles

```
# ============================================================
# SCRIPT TO MODIFY THE DSSAT SOIL PARAMETERS
# JUN 10, 2022
# ============================================================
# SOIL PROFILE FRAME TO COMPLETE SOL FILE FOR ENTIRE FIELD (BJERTOP)

setwd('D:\\Mes documents\\2021-2022 SLU\\4. Master thesis\\DSSAT\\Soil\
\SOL_file')
dir()

#prepare master file : add latitude, longitude, parameters to change
#create the parameter table in csv (carefull with the number of digits)

# --- reading the "master" files
mf = readLines("Soil_profile_frame.SOL") #incomplete line found on the file
is normal
#mft <- data.frame()

# --- list of parameters to be changed
# Careful with the number of digits available (to be changed in Excel)
param_list <- read.table("YieldTable.csv", header = FALSE, sep = ";")


# you can either read an external csv file with all parameters you want to
change,
# as well as other names, like city, plot number, ..., which maybe can be
included to name
# of the modified file.
# but the most important is to be sure that the all parameters you want to
change are
# some how indicated in the "master file".

print (param_list)

 #for(l in 2:ncol(param_list)){ #1st column is headers so we start with 2
 # text_col <- data.frame(NA,l)              # Creating new variable
 # data[ , i] <- new_col                     # Adding new variable to data
  #colnames(data)[i] <- paste0("Col_", i)    # Renaming new variable
#}

c= ncol(param_list)-1
r=length(mf)
mft <- matrix(nrow = r, ncol = c, data = mf) #r is the number of rows in
each soil profile
temp_soil_file <- matrix(nrow = r, ncol = c, data=NA)
tf <- matrix(nrow = r, ncol = c, data=NA)

#number of rows from soil profile and number of columns from param_list
#creates a matrix with the right number of soil profiles

for(l in (2:ncol(param_list))-1){ #number of columns whitout accounting for
the parameters' names nor soil profile 1
  for(k in 1:nrow(param_list)){
    if(k == 1){ # 1st interation
      temp_soil_file[,l] <- gsub(pattern = param_list[k,1], #parameters'
names are in column 1
                          replace = param_list[k,l+1],#values are in
columns 2
```

```
                          x = mft[,l])
      writeLines(temp_soil_file[,l], paste0('D:\\Mes documents\\2021-2022
SLU\\4. Master thesis\\DSSAT\\Soil\\SOL_file/soil_profile1.SOL'))
      # make sure to use the same file name

    }else{ # 2nd, 3rd,...,n interactions, but do not need to care about it
      tf[,l] <- readLines(paste0('D:\\Mes documents\\2021-2022 SLU\\4.
Master thesis\\DSSAT\\Soil\\SOL_file/soil_profile1.SOL'))
      # make sure to use the same file name
      temp_soil_file[,l] <- gsub(pattern = paste(param_list[k,1]),
                          replace = paste(param_list[k,l+1]),
                          x = tf[,l])
      writeLines(temp_soil_file[,l], paste0('D:\\Mes documents\\2021-2022
SLU\\4. Master thesis\\DSSAT\\Soil\\SOL_file/soil_profile1.SOL'))
      # make sure to use the same file name

    }

    if(k == 9) { #nrow(param_list))
      print (paste0('the ', l, ' soil profile is done!'))
    }#else{
      #print ("end")
  }
}

#print(temp_soil_file)

FieldAB_all <- c(temp_soil_file) #converts matrix into successive lines

#print(soil_profile_all)
writeLines(FieldAB_all, paste0('D:\\Mes documents\\2021-2022 SLU\\4. Master
thesis\\DSSAT\\Soil\\SOL_file/FieldAB_all.SOL'))

#careful with the number of digits ... the soil profile may not work
```

Appendix 2: Examples of soil profiles

```
*SEBJT0001    SWE   SandyLoam   200    ISRIC soilgrids + HC27
@SITE        COUNTRY          LAT     LONG SCS Family
 -99             SE       58.226   13.116     HC_GEN0011
@ SCOM  SALB  SLU1  SLDR  SLRO  SLNF  SLPF  SMHB  SMPX  SMKE
    BK  0.10  6.00  0.50 75.00  1.00  1.00 SA001 SA001 SA001
@  SLB  SLMH  SLLL  SDUL  SSAT  SRGF  SSKS  SBDM  SLOC  SLCL  SLSI  SLCF  SLNI  SLHW  SLHB  SCEC  SADC
     5 A     0.175 0.297 0.440  1.00  2.91  1.37  2.38 34.00 59.00 -99.0  0.21  6.50 -99.0  15.1 -99.0
    15 A     0.075 0.178 0.387  0.85  2.58  1.38  6.45 12.31 31.43 -99.0  0.09  5.65 -99.0  13.2 -99.0
    30 AB    0.085 0.190 0.387  0.70  2.16  1.41  4.92 14.11 30.49 -99.0  0.07  5.75 -99.0  12.9 -99.0
    60 BA    0.098 0.202 0.387  0.50  1.75  1.46  3.15 16.25 29.27 -99.0  0.06  5.86 -99.0  13.4 -99.0
   100 B     0.097 0.200 0.386  0.38  1.80  1.52  1.83 16.15 28.56 -99.0  0.05  6.00 -99.0  13.4 -99.0
   200 BC    0.088 0.188 0.385  0.05  2.13  1.57  1.05 14.72 28.04 -99.0  0.05  6.18 -99.0  13.4 -99.0

*SEBJT0002    SWE   SandyLoam   200    ISRIC soilgrids + HC27
@SITE        COUNTRY          LAT     LONG SCS Family
 -99             SE       58.226   13.116     HC_GEN0011
@ SCOM  SALB  SLU1  SLDR  SLRO  SLNF  SLPF  SMHB  SMPX  SMKE
    BK  0.10  6.00  0.50 75.00  1.00  1.00 SA001 SA001 SA001
@  SLB  SLMH  SLLL  SDUL  SSAT  SRGF  SSKS  SBDM  SLOC  SLCL  SLSI  SLCF  SLNI  SLHW  SLHB  SCEC  SADC
     5 A     0.183 0.294 0.443  1.00  2.91  1.36  2.44 36.00 58.00 -99.0  0.19  6.50 -99.0  15.1 -99.0
    15 A     0.075 0.178 0.387  0.85  2.58  1.38  6.45 12.31 31.43 -99.0  0.09  5.65 -99.0  13.2 -99.0
    30 AB    0.085 0.190 0.387  0.70  2.16  1.41  4.92 14.11 30.49 -99.0  0.07  5.75 -99.0  12.9 -99.0
    60 BA    0.098 0.202 0.387  0.50  1.75  1.46  3.15 16.25 29.27 -99.0  0.06  5.86 -99.0  13.4 -99.0
   100 B     0.097 0.200 0.386  0.38  1.80  1.52  1.83 16.15 28.56 -99.0  0.05  6.00 -99.0  13.4 -99.0
   200 BC    0.088 0.188 0.385  0.05  2.13  1.57  1.05 14.72 28.04 -99.0  0.05  6.18 -99.0  13.4 -99.0

*SEBJT0003    SWE   SandyLoam   200    ISRIC soilgrids + HC27
@SITE        COUNTRY          LAT     LONG SCS Family
 -99             SE       58.226   13.116     HC_GEN0011
@ SCOM  SALB  SLU1  SLDR  SLRO  SLNF  SLPF  SMHB  SMPX  SMKE
    BK  0.10  6.00  0.50 75.00  1.00  1.00 SA001 SA001 SA001
@  SLB  SLMH  SLLL  SDUL  SSAT  SRGF  SSKS  SBDM  SLOC  SLCL  SLSI  SLCF  SLNI  SLHW  SLHB  SCEC  SADC
     5 A     0.161 0.285 0.421  1.00  2.91  1.32  2.61 31.00 55.00 -99.0  0.17  6.30 -99.0  15.1 -99.0
    15 A     0.075 0.178 0.387  0.85  2.58  1.38  6.45 12.31 31.43 -99.0  0.09  5.65 -99.0  13.2 -99.0
    30 AB    0.085 0.190 0.387  0.70  2.16  1.41  4.92 14.11 30.49 -99.0  0.07  5.75 -99.0  12.9 -99.0
    60 BA    0.098 0.202 0.387  0.50  1.75  1.46  3.15 16.25 29.27 -99.0  0.06  5.86 -99.0  13.4 -99.0
   100 B     0.097 0.200 0.386  0.38  1.80  1.52  1.83 16.15 28.56 -99.0  0.05  6.00 -99.0  13.4 -99.0
   200 BC    0.088 0.188 0.385  0.05  2.13  1.57  1.05 14.72 28.04 -99.0  0.05  6.18 -99.0  13.4 -99.0

*SEBJT0004    SWE   SandyLoam   200    ISRIC soilgrids + HC27
@SITE        COUNTRY          LAT     LONG SCS Family
 -99             SE       58.226   13.116     HC_GEN0011
@ SCOM  SALB  SLU1  SLDR  SLRO  SLNF  SLPF  SMHB  SMPX  SMKE
    BK  0.10  6.00  0.50 75.00  1.00  1.00 SA001 SA001 SA001
@  SLB  SLMH  SLLL  SDUL  SSAT  SRGF  SSKS  SBDM  SLOC  SLCL  SLSI  SLCF  SLNI  SLHW  SLHB  SCEC  SADC
     5 A     0.188 0.285 0.438  1.00  2.91  1.39  2.26 37.00 55.00 -99.0  0.18  6.50 -99.0  15.1 -99.0
    15 A     0.075 0.178 0.387  0.85  2.58  1.38  6.45 12.31 31.43 -99.0  0.09  5.65 -99.0  13.2 -99.0
    30 AB    0.085 0.190 0.387  0.70  2.16  1.41  4.92 14.11 30.49 -99.0  0.07  5.75 -99.0  12.9 -99.0
    60 BA    0.098 0.202 0.387  0.50  1.75  1.46  3.15 16.25 29.27 -99.0  0.06  5.86 -99.0  13.4 -99.0
   100 B     0.097 0.200 0.386  0.38  1.80  1.52  1.83 16.15 28.56 -99.0  0.05  6.00 -99.0  13.4 -99.0
   200 BC    0.088 0.188 0.385  0.05  2.13  1.57  1.05 14.72 28.04 -99.0  0.05  6.18 -99.0  13.4 -99.0

*SEBJT0005    SWE   SandyLoam   200    ISRIC soilgrids + HC27
@SITE        COUNTRY          LAT     LONG SCS Family
 -99             SE       58.226   13.116     HC_GEN0011
@ SCOM  SALB  SLU1  SLDR  SLRO  SLNF  SLPF  SMHB  SMPX  SMKE
    BK  0.10  6.00  0.50 75.00  1.00  1.00 SA001 SA001 SA001
@  SLB  SLMH  SLLL  SDUL  SSAT  SRGF  SSKS  SBDM  SLOC  SLCL  SLSI  SLCF  SLNI  SLHW  SLHB  SCEC  SADC
     5 A     0.175 0.294 0.438  1.00  2.91  1.39  2.26 34.00 58.00 -99.0  0.21  6.50 -99.0  15.1 -99.0
    15 A     0.075 0.178 0.387  0.85  2.58  1.38  6.45 12.31 31.43 -99.0  0.09  5.65 -99.0  13.2 -99.0
    30 AB    0.085 0.190 0.387  0.70  2.16  1.41  4.92 14.11 30.49 -99.0  0.07  5.75 -99.0  12.9 -99.0
```

Appendix 3: Genetic coefficients generated by DSSAT crop models

```
$CULTIVARS:BACER047

! Coefficients used in the Cropsim-Ceres model differ from those used
! in DSSAT Version 3.5 AND 4.0. They can be calculated (approximately) from
! V3.5 coefficients as follows:

! P1V   = P1V(v3.5)*10
! P1D   = P1D(V3.5)*20
! P5    = P5(V3.5)*20 + 430
! G1    = G1(V3.5)*5 + 5
! G2    = (G2(V3.5)*0.35+0.65) * P5/20
! G3    = G3(V3.5)*0.7
! PHINT = PHINT(V3.5)

! Converted coefficients,and those listed below,should always be
! tested by using them with real experiments and comparing model
! outputs with measured values.

*CULTIVARS:BACER047
@VAR#  VAR-NAME........  EXP#   ECO#   P1V   P1D    P5    G1    G2    G3 PHINT
IB0031 Juliette Nguyen      . DFAULT 9.155 30.99 940.5 35.78 49.95 6.920 60.00

! COEFF       DEFINITION
! ========    ==========
! VAR#        Identification code or number for the specific cultivar.
! VAR-NAME    Name of cultivar.
! EXP#        Number of experiments used to generate parameters
! ECO#        Ecotype code for this cultivar,points to entry in ECO file
! P1V         Days,optimum vernalizing temperature,required for vernalization
! P1D         Photoperiod response (% reduction in rate/10 h drop in pp)
! P5          Grain filling (excluding lag) phase duration (oC.d)
! G1          Kernel number per unit canopy weight at anthesis (#/g)
! G2          Standard kernel size under optimum conditions (mg)
! G3          Standard,non-stressed mature tiller wt (incl grain) (g dwt)
! PHINT       Interval between successive leaf tip appearances (oC.d)
```

```
$ECOTYPES:BACER047

! Coefficients presented here differ from those used in DSSAT
! Version 3.5. They have been developed from 'parameters'
! embedded in the code of the Ceres model,from the Cropsim model,
! and from the literature. They are likely to change as more
! experience is gained, and should not yet be taken as fixed.

! In Ceres3.5, P1=400 for PHINT=95; P2=phint*3; P3=phint*2; P4=200,
! with anthesis occurring in P4 after 80 units.

*ECOTYPE:BACER047
!         ------PHENOLOGY(PHASE_DURATIONS)------ P.MOD --MAX_RUE--  LEAF PRODN  ------LEAF_SIZES------ LEAF_SENESC TILLER_PRODUCTION ---TILLER_DEATH-- ROOTS -----CANOPY------  ---COMPOSITION--  KILL
@ECO#     P1 P2FR1    P2    P3 P4FR1 P4FR2    P4  VEFF PARUE PARU2  PHL2  PHF3  LA1S  LAFV  LAFR  SLAS LSPHS LSPHE TIL#S TIPHE TIFAC TDPHS TDPHE TDFAC  RDGS HTSTD  AWNS  KCAN  RS%S  GN%S GN%MN  TKFH
DFAULT   200   .25   200   200  0.25  0.10   200   0.6   2.7   2.7    15   1.3   5.0  0.10  0.50   400   5.5   6.3   3.5   2.5   1.0   2.5   6.0   4.0   3.0   100   0.0   .85    30   3.0   0.0   -10

! COEFF   DEFINITION
! =====   ==========
! AWNS    Awn score (0-10;10=very long)
! ECO#    Code for the ecotype (code)
! GN%MN   Minimum grain N (%)
! GN%S    Standard grain N (%)
! HTSTD   Standard canopy height (cm)
! KCAN    PAR extinction coefficient (#)
! LA1S    Area of standard first leaf (cm2)
! LAFR    Increase in potential area of leaves,reproductive phase (fr/leaf)
! LAFV    Increase in potential area of leaves,vegetative phase (fr/leaf)
! LARS    Area of standard reproductive phase leaf (cm2)
! LAVS    Area of standard vegetative phase leaf (cm2)
! LLIFE   Life of leaves during vegetative phase (phyllochrons)
! LSPHE   Final leaf senescence ends (GrowhStage)
! LSPHS   Final leaf senescence starts (GrowhStage)
! P1      Duration of phase end juvenile to terminal spikelet (PVTU)
! P2      Duration of phase terminal spikelet to end leaf growth (TU)
! P2FR1   Duration of phase terminal spikelet to jointing (fr P2)
! P3      Duration of phase end leaf growth to end spike growth (TU)
! P4      Duration of phase end spike growth to end grain fill lag (TU)
! P4FR1   Duration of phase end spike growth to anthesis (fr P4)
! P4FR2   Duration of phase anthesis start to anthesis end (fr P4)
! PARU2   PAR conversion to dm ratio,after last leaf (g/MJ) (If -99,set to PARUE)
! PARUE   PAR conversion to dm ratio,before last leaf stage (g/MJ)
! PHFn    Factor by which PHINTS is multiplied -> PHINT for phase (#)
! PHLn    Leaf # produced during phyllochron phase (#)
! PPFPE   Daylength factor,pre emergence (#,0-1)
! RDGS    Root depth growth rate,early phase (cm/standard d)
! RS%S    Reserves part of assimilates going to stem (%)
! SLAS    Specific leaf area,standard first leaf (cm2/g)
! TDFAC   Tiller death factor (%/st.day when tiller wt 2xstandard wt)
! TDPHE   Tiller death ending stage (GrowthStage)
! TDPHS   Tiller death start stage (GrowthStage)
! TIFAC   Tiller initiation (rate) factor (fr of phyllochron based) (#)
! TIL#S   Tiller production starts (leaf #)
! TIPHE   Tillering phase end stage (GrowthStage)
! TKFH    Temperature at which killed when fully hardened (oC)
! VEFF    Vernalization effect (Rate reduction when unvernalized (fr)
! WFGU    Water stress factor,growth,upper (fr)
! WFPU    Water stress factor,photosynthesis,upper (fr)
```

Publishing and archiving

Approved students' theses at SLU are published electronically. As a student, you have the copyright to your own work and need to approve the electronic publishing. If you check the box for **YES**, the full text (pdf file) and metadata will be visible and searchable online. If you check the box for **NO**, only the metadata and the abstract will be visible and searchable online. Nevertheless, when the document is uploaded it will still be archived as a digital file. If you are more than one author, the checked box will be applied to all authors. Read about SLU's publishing agreement here:

- https://www.slu.se/en/subweb/library/publish-and-analyse/register-and-publish/agreement-for-publishing/.

☒ YES, I/we hereby give permission to publish the present thesis in accordance with the SLU agreement regarding the transfer of the right to publish a work.

☐ NO, I/we do not give permission to publish the present work. The work will still be archived and its metadata and abstract will be visible and searchable.